Title

Synthesis, Water Adsorption Behavior of Zeolite NaY and Investigation on Energy-conserving NaY Composites

Author

Yang, Zhuoqi

Publication Date

2021

Peer reviewed|Thesis/dissertation

Synthesis, Water Adsorption Behavior of Zeolite NaY and Investigation on Energy-conserving NaY Composites

By

ZHUOQI YANG

THESIS

Submitted in partial satisfaction of the requirements for the degree of

MASTER OF SCIENCE

in

Chemistry

in the

OFFICE OF GRADUATE STUDIES

of the

UNIVERSITY OF CALIFORNIA

DAVIS

Approved:

Susan Kauzlarich, Chair

Gang-yu Liu

Delmar Larsen

Committee in Charge

2021

Acknowledgement

I wish to express my most sincere appreciation to my advisor, Prof. Ting Guo. His guidance, patience, and suggestion helped me through all the stages of the project. In addition to academic research, his advice and support for my various difficulties was incredibly helpful. I would also like to thank my committee members, Prof. Susan Kauzlarich, Prof. Gang-yu Liu and Prof. Delmar Larsen for their time, suggestions, and encouragement.

All the members of Guo group made the study and work in the lab interesting and enjoyable. I know how fortunate I was to have such nice people as lab-mates. Dr. Jennifer Lien and Mengqi Su offered me indispensable help and encouragement. I would also like to thank Anthony Soukey and Aaron Stacy for their help with zeolite project. People I met at Guo lab and UC Davis will be in my heart with deep appreciation for their kindness and support. I would also like to express gratitude to our collaborators, Prof. Donadio and Dr. Shunda Chen for their excellent work in theoretical simulations, as well as Prof. Chandrasekar and Dr. Francesc Junyent for their technical support. Also, I would like to acknowledge the McClellan Nuclear Research Center and Dr. Wesley Frey for the neutron imaging.

Finally, I thank my family for their understanding and encouragement, I was able to overcome physically and emotionally hard times due to their support. I would also like to give sincere and special thanks to my precious, Boston and my partner Chengyang, for their love and support along the way.

Abstract

In this work, microsized zeolite NaY was synthesized using a hydrothermal method with sodium silicate as the silicone source without the organic template. The chemical composition of reaction gel was determined, preparation of the precursor and the reaction conditions for hydrothermal reaction were studied and optimized. The reason for the production of side product Na-P1 was proposed and discussed.

As a promising desiccant for wide applications, the water adsorption behavior of NaY and commercial Y type zeolite was investigated. Proton solid-state NMR spectra were used to investigate the bonding in the framework for different hydration standards of zeolite samples. Neutron images were taken to explore the hydration and dehydration pattern and diffusion style of bulk zeolite samples. The dehydration of the commercial and synthesized NaY zeolites was also explored. Finally, the composites of NaY zeolite and other types of materials, glass and polyurethane were designed and investigated, and could potentially be used for reproducible water adsorption process and work as energy-conserving material.

TABLE OF CONTENTS

Chapter 1 Zeolite Faujasite hydrothermal synthesis

1.1 Introduction

Alex Fredrik Cronstedt, a Swedish mineralogist, first identified zeolite as a mineral in 1756 when he collected several crystals from a copper mine. He discovered that fast heating the substance stilbite will generate a large volume of steam from water and the steam is absorbed by the material. Because of its capacity to froth when heated to roughly 200 ℃, he named the substance zeolite, which comes from Greek words meaning "boiling stones."[1] Natural zeolites are formed when alkaline groundwater reacts with volcanic rocks and ash deposits. Zeolites can also form in post depositional environments over timescales from thousands to millions of years in shallow oceanic basins. However, natural zeolites are rarely pure, they are easily contaminated to different degrees by other minerals, metals, crystalline silica, and other substances.[2] Therefore, naturally formed zeolites are omitted from various important commercial applications which requires uniformity and pureness.

Zeolite is defined by Coombs et al. as a crystalline aluminosilicate substance with a tetrahedral framework linked structure, each contains four oxygen atoms encompassing a cation.[3] This framework contains open cavities formed by various channels and cages. Cavities can be occupied by water molecules. The channels' size is large enough to let external molecules to pass through and can also be suitable to hold molecules.

Zeolites were first successfully synthesized by Barrer in the 1940s. There are around 50 different types of zeolites identified and more types were being synthesized and investigated. The morphological features, crystal structure, chemical composition, pore and channel diameter, natural occurrence, etc. have all been used to classify zeolites. One of the most essential features of zeolite is Silicon/Aluminum ratio. The Si/Al ratio is straight proportional to

the thermostability but conversely proportional to the cation content. Moreover, with the development of zeolite applications in industries and labs for catalysis, ion exchange, separations and adsorptions, the pore and channel structure of zeolite has public appeal and been studied in recent years.

The zeolite Faujasite (FAU) has one of the most open silicate frameworks among the known zeolites currently and it has a wide range of Si/Al ratio. As shown in Figure 1.1, the Faujasite framework structure has 1.3 nm diameter supercages which is bridged by twelve-membered silicate rings. Each unit cell is composed of 8 supercages, 16 double six-membered rings (D6R), 16 twelve-membered ring, 32 single six-membered rings (S6R) and 8 sodalite cavities.[4] Up to 260 water molecules per unit cell can be held in this open framework, varying based on the Si/Al ratio and potential cation sites, which shows the large internal space capacity.[5] More detailed information about zeolite crystalline structures can be found at the International Zeolite Association database.

Faujasite is classified into Faujasite X and Y based on their Si/Al ratio, generally, except the dealuminated Faujasite, X has the Si/Al ratio <1.5 and Y is >1.5, high silica Y has the ratio >3.0, the conversion of X to Y modification can happen at a Si/Al ratio of 1.5. The framework has neutral SiO_2 groups and negative charges groups AlO_2^- , which are balanced by the positive charged cations such as Na^+, NH_4^+, Li^+, K^+, Ca^{2+}, and so on in the non-framework positions. This enable the Faujasite to be a popular ion-exchange medium and also works as a catalyst and absorbent.

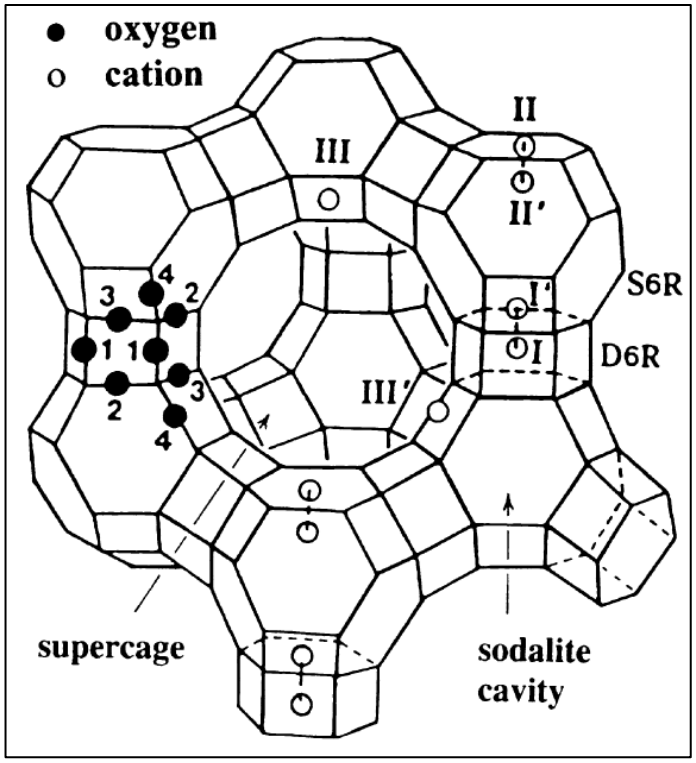

Figure1.1. Faujasite zeolite stylized framework and its cation sites. The structure is distinguished by its supercages, hexagonal prism and sodalite cavity.[4] Reproduced with permission from J. M. Lee.

Zeolite Faujasite A and X was industrial manufactured by Milton in 1959,[6] then Breck successfully synthesized Y zeolite in 1964.[7] The synthesis of Faujasite NaY had appealed a lot attention in recent years because it plays a crucial role in petrochemistry area. Also, many efforts have been devoted to the applications of NaY, and it's been reported that NaY can be used in antibacterial studies,[8] waste treatment,[9] photocatalytic reactions,[10] anticancer therapies,[11] etc. Possessing high surface-to-atom ratio and large surface area, microsized NaY has attracted a great deal of attention due to its applications in the abovementioned studies and many other exploitable areas. Previous investigations on factors affecting zeolite formation indicates that the chemical composition of reaction mixture, preparation of precursor solution, mixing of precursor and reaction solution, aging condition of precursor solution and hydrothermal reaction temperature and time will all

affect the crystallization of microsized NaY.[12] The use of organic templates to drive the synthesis of microsized zeolites is common in many synthesis routes, though the majority of organic templates need to be calcinated at high temperature to be fully removed which requires a lot of time and energy.[13] At the same time, the toxic and volatile organic template will produce harmful exhaust gas which is incompatible with green chemistry. Thus, the investigation of inorganic precursor solution to provide nuclei for zeolite synthesis is necessary. Therefore, to make the syntheses more convenient and economic, less expensive inorganic silica sources has been explored and used in current NaY syntheses.[14]

In this work, microsized zeolite NaY was synthesized with sodium silicate as the silicone source without organic template using hydrothermal method. The chemical composition of reaction mixture was determined, preparation of the precursor and reaction mixture and the reaction conditions for hydrothermal reaction was optimized. Pure Zeolite P was also synthesized by coincidence when investigating the aging condition of the precursor solution.

1.2 Experimental

1.2.1 Materials and synthesis

The silicone source used for Faujasite NaY synthesis were reagent grade sodium silicate solution (Na_2O, ~10.6%; SiO_2, ~26.5%, Sigma-Aldrich). Sodium hydroxide (Fisher Scientific), sodium aluminate (technical, anhydrous, Sigma-Aldrich) and deionized water were also used in the syntheses of NaY zeolite.

The synthesis mixture molar composition was modified based on bibliography.[15] To make the precursor mixture, sodium hydroxide was dissolved in deionized water, then sodium aluminate

was added. Above solution was added to sodium silicate solution under room temperature with stirring. The precursor solution was aged at different temperature for different duration until the solution converted to white translucent gel. The precursor solution was prepared by the composition of 16.0 Na_2O: 1.0 Al_2O_3: 14.0 SiO_2: 300 H_2O.

Afterwards, anhydrous sodium aluminate was dissolved in deionized water and added into sodium silicate solution under vigorous mechanical stirring quickly. Then a certain amount of precursor gel was added to the mixture subsequently. The mixture was transferred to a Teflon autoclave until the mixture became viscous and uniform and the composition for the final gel was 66.5 Na_2O: 1.0 Al_2O_3: 150 SiO_2: 3200 H_2O. The autoclave was put in an oven preheated to 373 K and heated for 24 h. The reaction was stopped by cold water quenching and the samples were collected by filtration and wash with deionized water. The filtrate was tested until reach pH = 8.

1.2.2 Characterization

Powder samples were obtained by grinding using mortar and pestle followed by drying in the furnace under temperature >473 K overnight. The crystalline structures of synthesized dried samples were determined by X-ray powder diffraction (XRD, Bruker D8 Eco) with Cu Kα radiation (λ = 1.5418 Å) operated at 40 kV and 25 mA. The samples were mounted on a zero-background holder and diffraction patterns were scanned over the range of 2–50° in 2θ scale with a step size increment of 0.02°. The average size and solid morphology of the zeolite particles was confirmed by scanning electron microscopy (SEM, FEI Scios 2 DualBeam) equipped with an energy dispersion spectroscopy (EDS). The silicone to aluminum ratio was measured using EDS. Samples for SEM and EDS were prepared, images were acquired by Dr. Jennifer Lien.

1.3 Results and discussion

The hydrothermal synthesis of Faujasite NaY is an inorganic reaction process, the purity and morphology of the product is controlled by the preparation of precursor, reaction conditions of reaction gel and hydrothermal crystallization temperature. For the same composition of the precursor and final reaction gel, above mentioned factors can lead to different product size and crystallinity.

The precursors, or structure directing agents (SDA) are used for facilitating the formation of channels and pores for the synthesis of zeolite. Various SDA have been applied for the synthesis of microsized Faujasite NaY. Organic SDA, also known as organic template, such as Tetrabutylammonium hydroxide (TBAOH)[16] and Tetraethylammonium hydroxide (TEAOH)[17] have been used for nanosized sized NaY synthesis. Organic template can also increase the Si/Al ratio which will further stabilize the NaY.[18] However, the post-synthesis calcination which cost a lot of time and energy and produce pollutant is becoming the main drawback of the use of organic SDA. Inspired by W. Bo,[15] an easy-to-make precursor gel was prepared in this experiment and the aging time and temperature effects was investigated for NaY formation. For aging time, 5 min, 1 h, 24 h, and 48 h was applied for the preparation of the inorganic precursor with same composition of 16.0 Na_2O: 1.0 Al_2O_3: 14.0 SiO_2: 300 H_2O. As shown in Figure 1.2, pure zeolite particles were made with the shortest aging time of 5 min. The Si/Al ratio was confirmed by SEM-EDS which is 1.69. Compared to Figure 1.3 and Figure 1.4, it is obvious that the zeolite particle morphologies are quite different, as well as the bulk sample status in Figure S6 which mainly due to the various size of the particles. It shows a spherical morphology in Figure 1.2 which is quite differ from Faujasite morphology, while it shows an irregular morphology which is consistent with Faujasite morphology in Figure 1.4 with the aging time of 24 h and 48 h. The blend of two morphologies is

observed in Figure 1.3 with the aging time of 1 h. The morphology change of the particles in the Figures indicates a trend of phase transformation from spherical to irregular as the aging time increased. When 5 min of aging time was applied, it turned out to be Na-P1, which is one of the members of the Gismondine group and is also known as another category of zeolite. The morphology of zeolite P made is consistent with the literature as shown in Figure S2.[19] To further confirm the composition of the particle, powder X-ray diffraction pattern was compared with the literature (Figure S2, S4). The synthesized Na-P1 particles have peaks at {1 1 0}, {2 0 0}, {2 1 1}, {3 1 0}, {3 2 1}, {4 3 1}, which agrees with the XRD pattern of literature and IZA zeolite database.

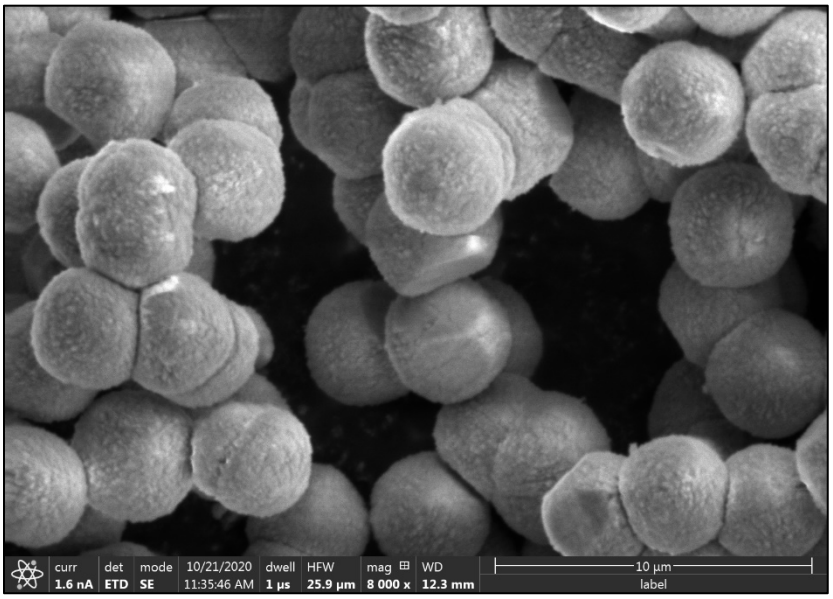

Figure 1.2. SEM image of synthesized zeolite particle using the SDA aged for 5 min under room temperature. The average size of zeolite particle is 4 ± 0.2 μm.

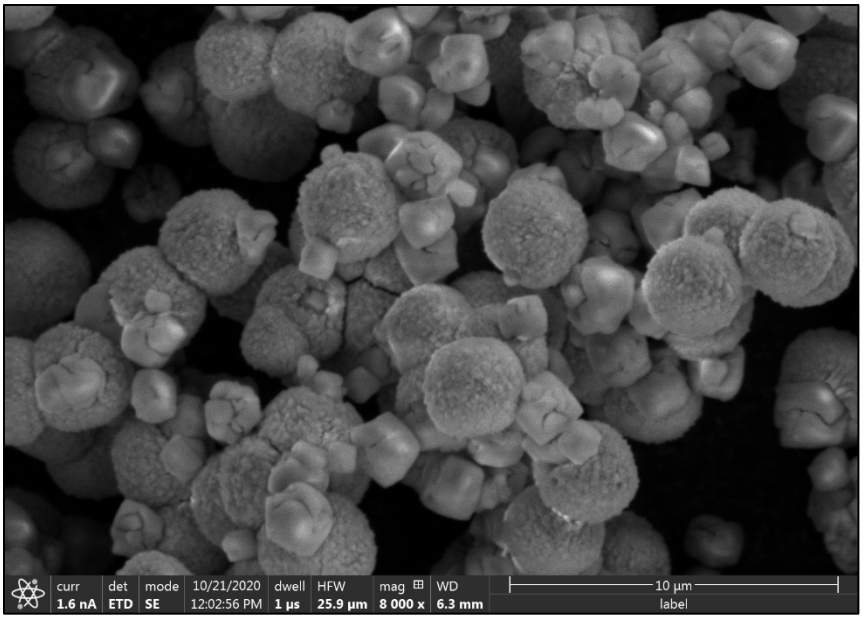

Figure 1.3. SEM image of synthesized zeolite particle using the SDA aged for 1 h under room temperature. The average size of zeolite P particle is 3 ± 0.2 μm, average size of zeolite Faujasite is 1.5 ± 0.8 μm.

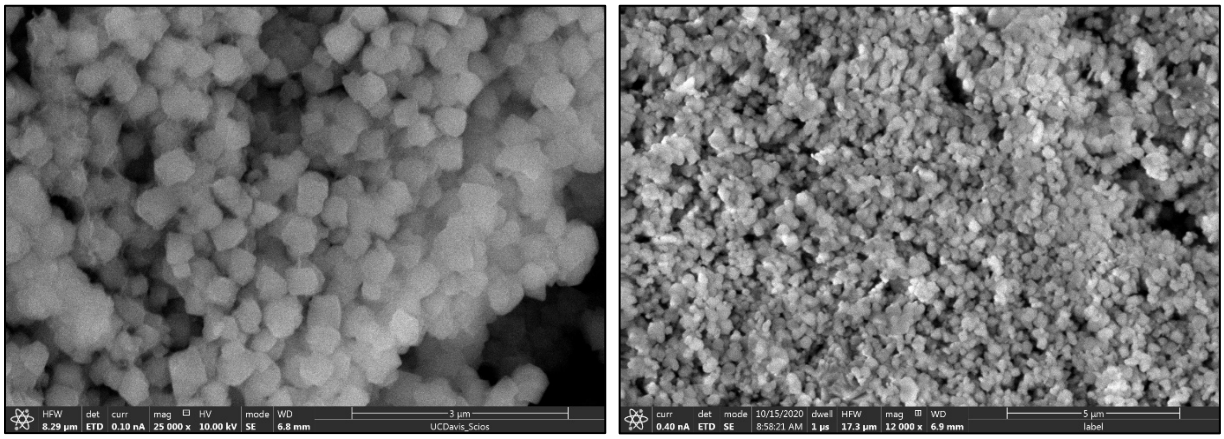

Figure 1.4. SEM images of synthesized zeolite NaY particles. Left: the synthesized particles with the SDA aged for 24 h, right: the particles with the aging time of 48 h. The scale bar for both images is 5 μm, and the particle size in left image is 350 nm, in right is 150 nm.

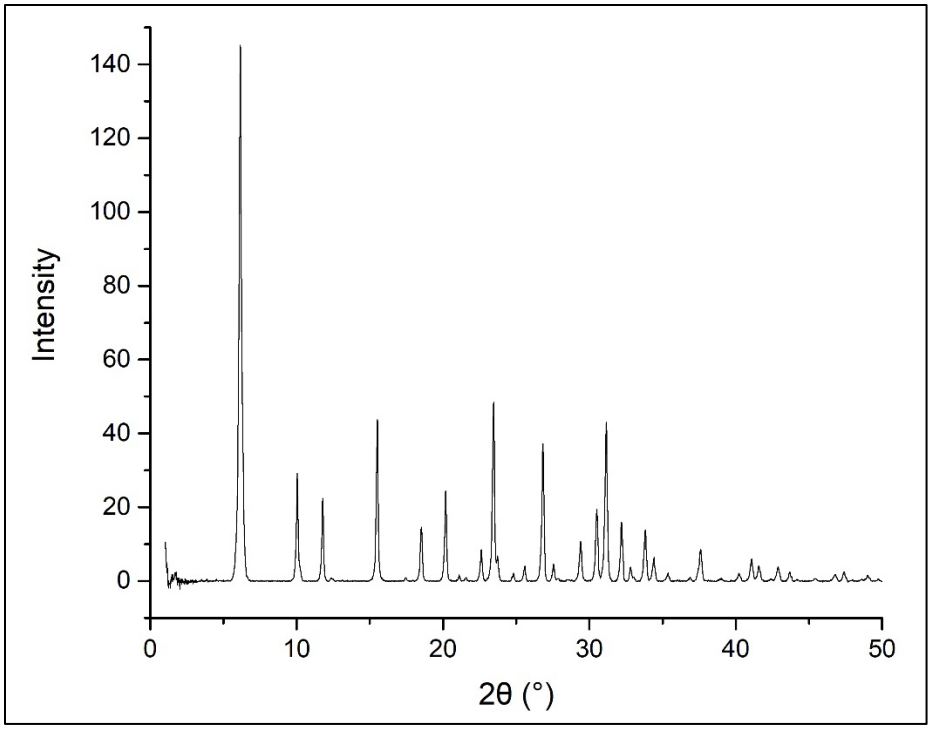

Figure 1.5. The powder X-ray diffraction pattern of zeolite NaY made by SDA with the aging time of 24 h.

For the 24 h aging particle sample, powder XRD pattern was obtained in Figure 1.5 to be compared with the literature (Figure S1). It can be noticed both patterns have the characteristic peaks at {1 1 0}, {2 2 0}, {3 1 1}, {3 3 1}, {4 4 0}, {5 3 3}, {6 4 2} and {5 5 5}, which can help to confirm the composition of 24 h aging zeolite particles is Faujasite. SEM image in Figure 1.4 is also strong evidence for the existence of Faujasite, and the EDS results shows Si/Al ratio is 2.3, which meets the criterial of Faujasite Y that Silicone to Aluminum ratio larger than 1.5. Get back to shorter aging time, Figure S5 shows the quick scan of powder XRD pattern of the 1 h aging sample. There is evidence of mixing peaks indicating the presence of two type of zeolite particles. There are peaks at {1 1 1}, {2 2 0}, {1 1 0}, {3 3 1}, {2 1 1}, {3 1 0} and {5 3 3} which belong to the characteristic peaks of above mentioned two types of zeolites, which indicates the sample is the mixture of NaY and zeolite P. The mixing of spherical and irregular morphology in Figure 1.3

validates the blending of NaY and zeolite P. It has been reported in the literature that the transformation of zeolite P to NaY can happen when hydrothermal crystallization temperature changed.[19] Zeolite P can also be formed as a side product when there is an absence of silica during Faujasite synthesis[20] or the sodium to aluminum ratio is increased.[21] Though the mechanism of the transformation hasn't been fully understood and there's no solid theory about the conversion and transformation, there is a possibility that zeolite P and Faujasite can be the side product for each other when changing the reaction condition. The aging time of SDA in this experiment, could be one of the factors affecting the conversion among these two zeolites. During the aging of SDA, the silicone source and aluminum source will form polymeric aluminosilicate species,[22] the oligomers formed will be the nuclei, or to say, "seeds" that to guide and facilitate crystal growth and formation. It has been verified by Thompson[23] and co-workers[24] that seeds formed offers sites for the secondary nucleation, and related study proved that there is monomer and dimer formed during the Faujasite NaX gel aging, higher oligomers (may up to Si_{20}) exist during the synthesis of siliceous Faujasite NaY.[25] Therefore, it can be proposed that when shorten the aging time, the formation of nuclei hasn't been started so there's no polymeric or even no monomer and dimer to support the nucleation of Faujasite that only Na-P1 is formed. When increasing the aging time to 1 h, part of the nuclei formed to guide the formation of Faujasite. While when becomes to 24 h, the nucleation of the original silicone and aluminum source is complete to an extent so there's no zeolite P formed as the side product. More aging time dependent synthesis and the design of separating gel and seed physically can be done for studying the mechanism and transformation time point.

When aging time of SDA becomes longer, which is 48 h in the experiment, NaY is still formed confirmed by the powder XRD pattern, only the size of the zeolite particle formed decreased from

350 nm to 150 nm. As stated above, the seed crystals work as nucleation center will form during the aging of SDA. More small crystallites may be released from the seed crystals during the grow of the seed crystals, which promote the complete nucleation of the SDA and the formation of smaller nuclei, thus leads to the smaller size particles formed after crystallization. Further studies can be done in the direction of aging time elongation and nanosized Faujasite synthesis.

It also been noticed that aging temperature is a factor that affecting the status of SDA and subsequent product formed. Three aging temperatures, 18 ℃, 25 ℃ (room temperature) and 30 ℃ were used for the NaY synthesis. It turned out the SDA aged well under 25 ℃ and 30 ℃, it transferred from a clear liquid to a viscous and semifluid gel as shown in Figure S7. Aging under 18 ℃ could be too low for the NaY synthesis since the gel stayed clear and the final product after crystallization is not unsized according to the SEM image in Figure 1.6. Presumably the temperature could be not high enough, so the growth of nuclei was slow and vary in speed which cause the size inconsistency. A rough microscope image was also taking for the SDA samples aged at 18 ℃ and 30 ℃ by using the lab made microscope as shown in Figure S8. Different areas were detected, and they indicate 18 ℃ aging results in numerous small different sized nuclei while 30 ℃ aging results in less and large sized nuclei, which may affect the subsequent crystallization.

Hydrothermal crystallization temperature was also investigated based on bibliography.[15,26] Two temperatures 90 ℃, and 100 ℃ were duplicated and applied for the hydrothermal reaction. As expected, the crystal size decreased to 200 nm under 90 ℃ compared to 350 nm under 100 ℃ which due to the slower speed of crystallization under lower temperature.

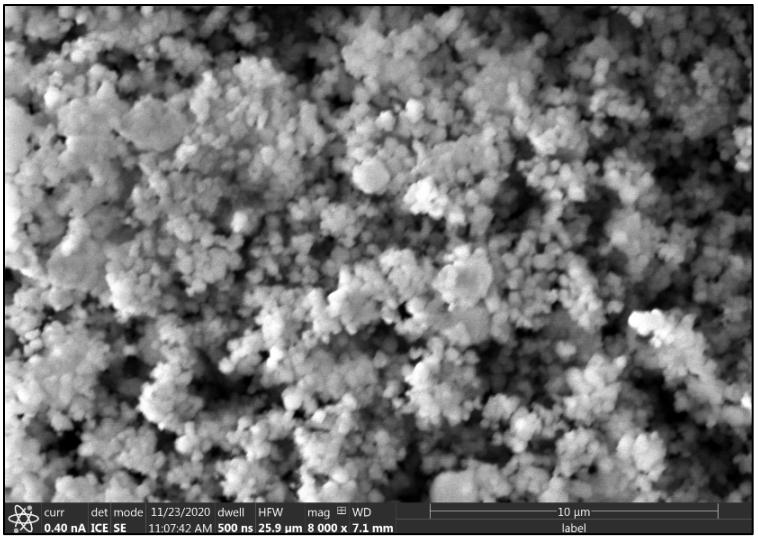

Figure 1.6. SEM image of synthesized zeolite particle using the SDA aged for 24 h under 18 ℃.

Overall, aging duration and aging temperature of the structure directing agent can control the formation of Faujasite NaY and zeolite P efficiently. Microsized pure NaY was successfully synthesized using SDA aged for 24 h under room temperature during hydrothermal reaction under 373 K heating for 24 h. Decrease the aging duration can facilitate the presence of side product in the form of zeolite P. The mechanism hasn't been clearly understood based on the current study and literature, related future work can enhance the understanding of hydrothermal synthesis mechanism with seeding method. And the decrease of the aging temperature reduces the number of nuclei formed and hydrothermal reaction temperature slow down the growth of NaY crystals, which can be further investigated for nanosized zeolite synthesis.

Appendix

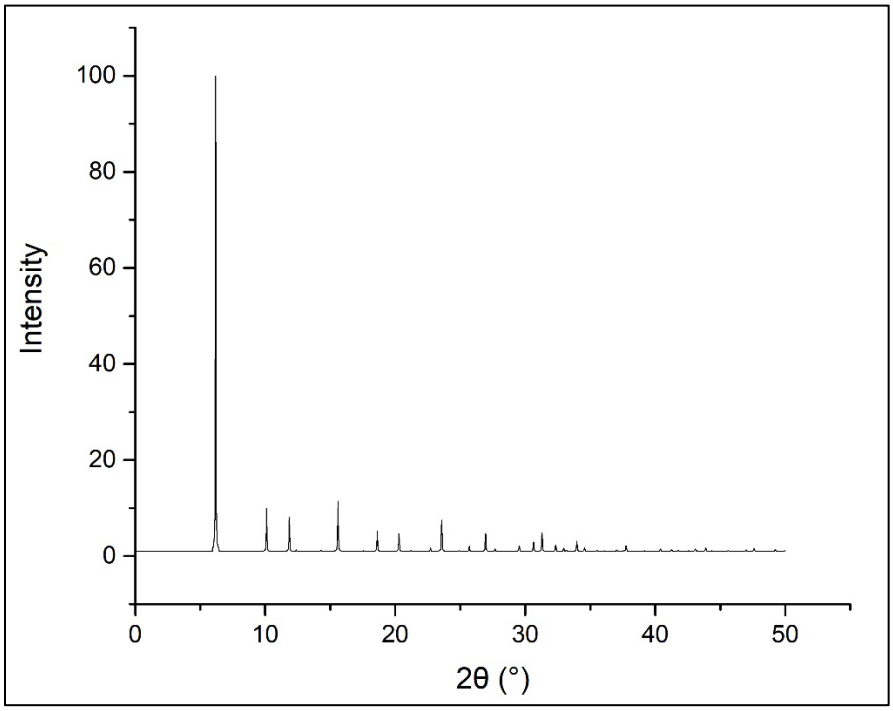

Figure S1. Powder X-ray diffraction patterns of Faujasite from the Database of Zeolite structures from the Structure Commission of the International Zeolite Association (IZA-SC).

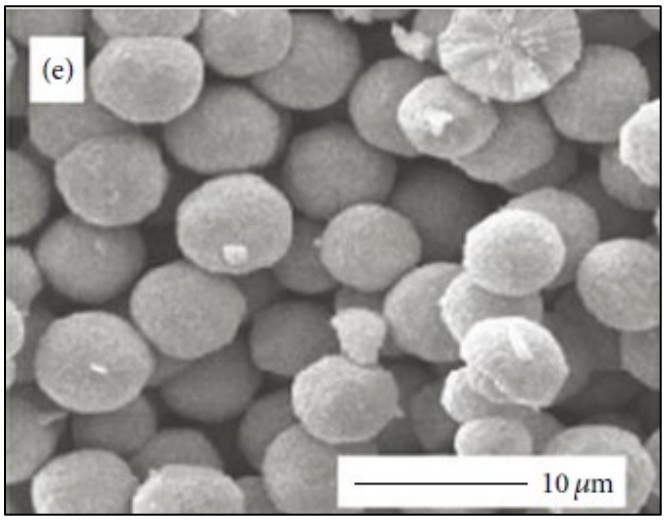

Figure S2. Scanning electron micrograph of synthesized zeolite P from literature. [19] Reproduced with permission from S. N. Azizi.

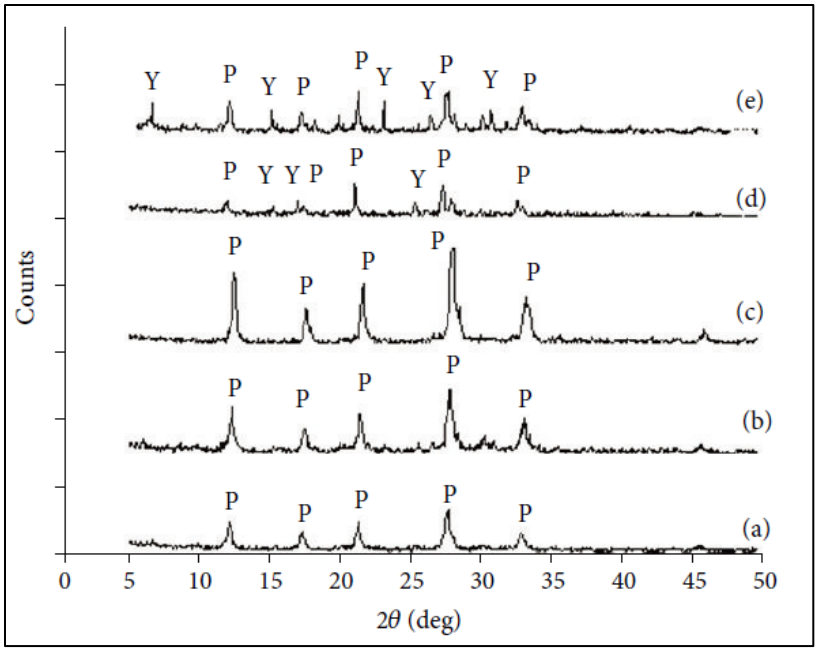

Figure S3. Powder X-ray diffraction patterns of synthesized zeolite P and zeolite Y with various Si/Al ratios from literature. [19] Reproduced with permission from S. N. Azizi.

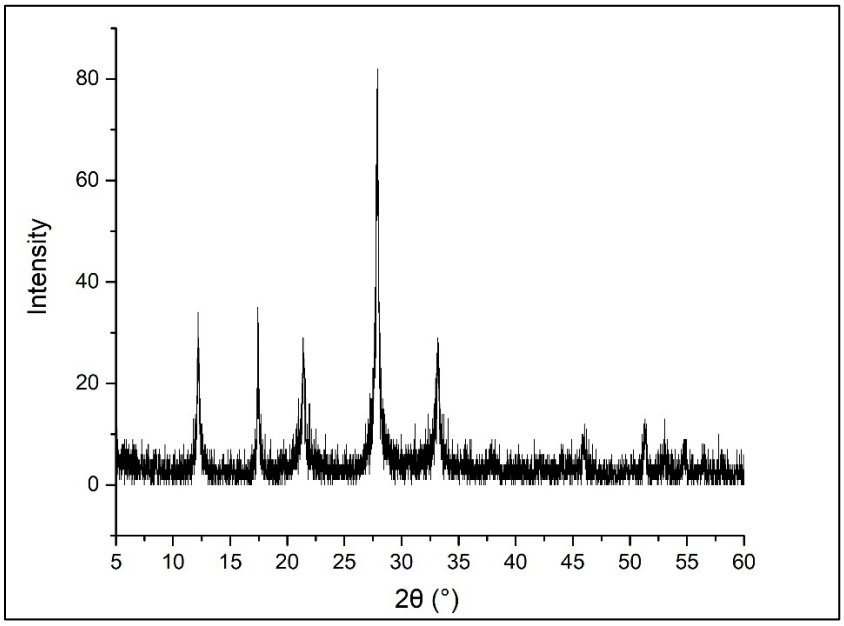

Figure S4. The quick scan of powder X-ray diffraction pattern of synthesized zeolite P with 5 min aging time.

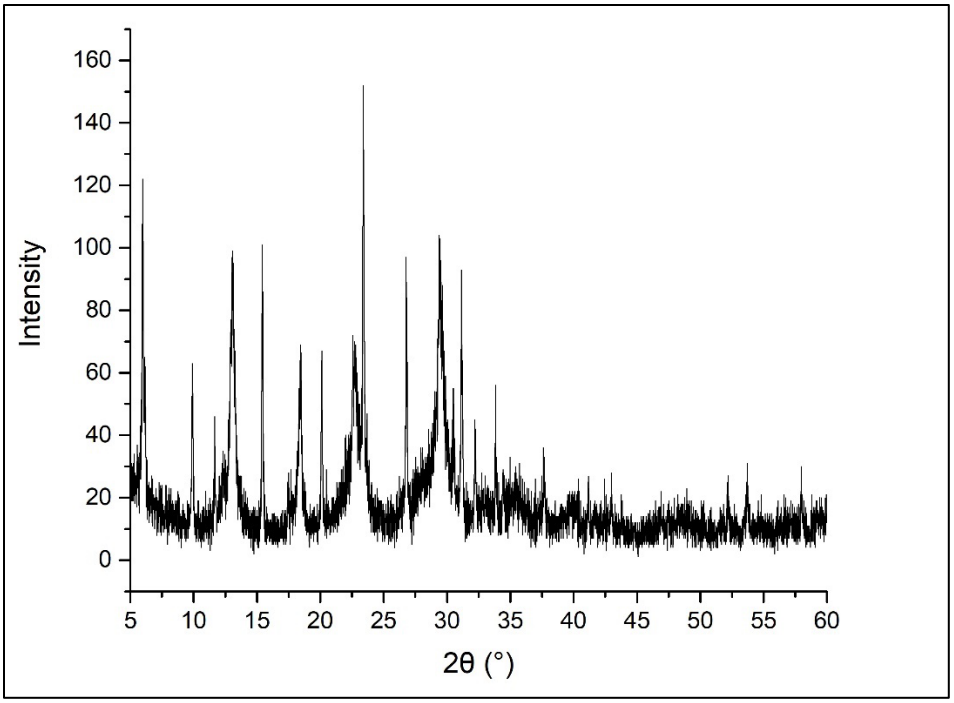

Figure S5. The quick scan of powder X-ray diffraction pattern of synthesized zeolite mixture with 1 h aging time.

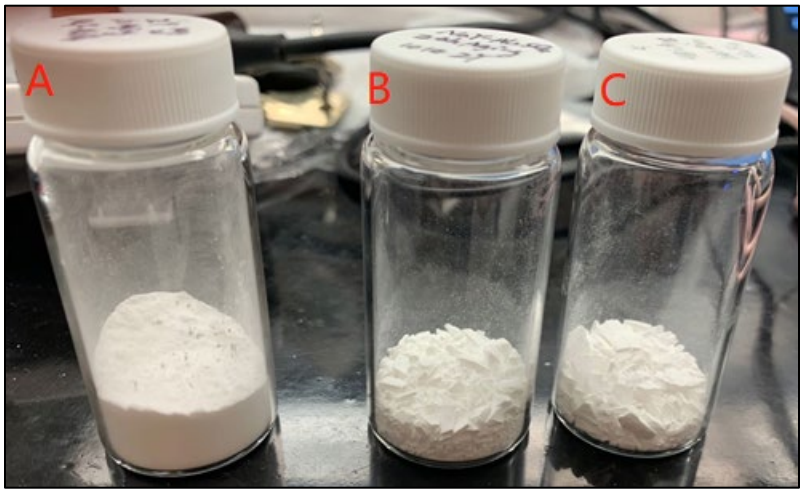

Figure S6. The photo of dried bulk synthesized zeolite particles without grinding. A: zeolite P with 1 h aging time of SDA; B: zeolite NaY with 24 h aging time; C: zeolite NaY with 48 h aging time.

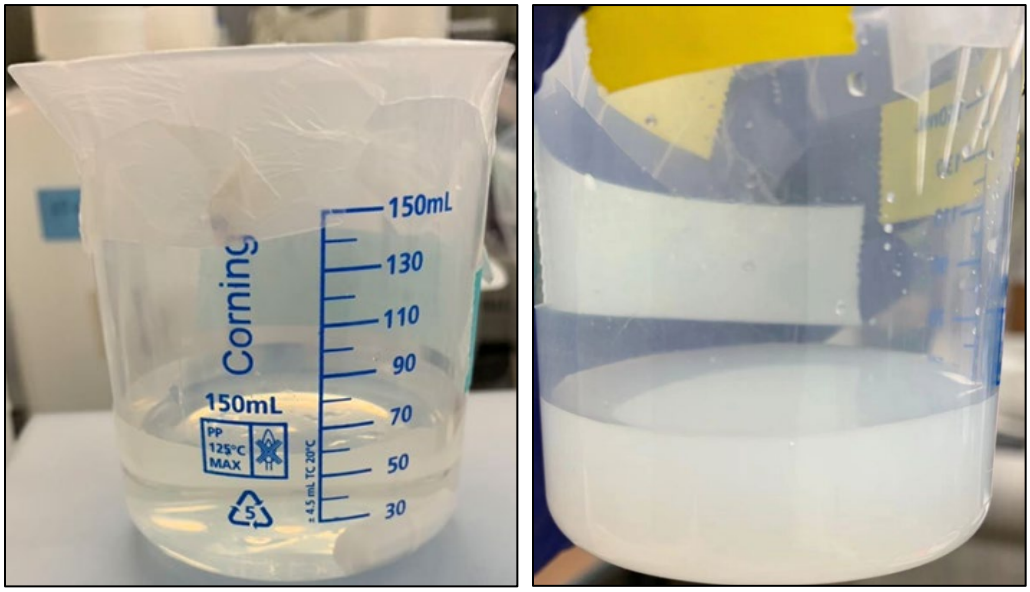

Figure S7. Photos of structure directing agent before (left) aging and after (right) 24 h aging.

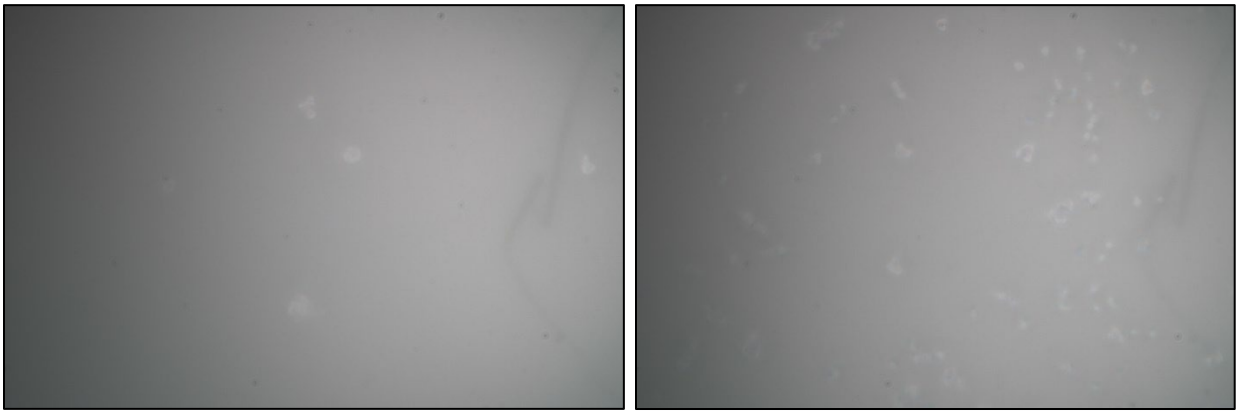

Figure S8. Pictures of structure directing agent aged at 18 ℃ and 30 ℃ by using the lab build microscope.

References

1. Reeve, P. J.; Fallowfield, H. J., Natural and surfactant modified zeolites: A review of their applications for water remediation with a focus on surfactant desorption and toxicity towards microorganisms. *J Environ Manage* **2018,** *205*, 253-261.
2. Ramesh, K.; Reddy, D. D., Zeolites and Their Potential Uses in Agriculture. **2011**; 219-241.
3. Douglas S. Coombs, Recommended Nomenclature for Zeolite Minerals. *The Canadian Mineralogist* **1998**, 62(4), 533-571.
4. Lee, J. M.; Seo, S. M.; Suh, J. M.; Lim, W. T., Synthesis and single-crystal structures of fully dehydrated fully Sr^{2+}-exchanged zeolite Y (FAU) and its benzene sorption complex. *Journal of Porous Materials* **2010**, 18 (5), 523-534.
5. Werner H. Baur; On the cation and water positions in faujasite. *American Mineralogist* **1964**, 49 (5-6): 697–704
6. R. M. Milton, Molecular sieve adsorbents, U.S. Patent 2882243, **1959**.
7. D.W. Breck, Crystalline zeolite Y, U.S. Patent 3130007, **1964**.
8. L. Ferreira, J.F. Guedes, C. Almeida-Aguiar, A.M. Fonseca, I.C. Neves, Microbial growth inhibition caused by Zn/Ag-Y zeolite materials with different amounts of silver Colloids *Surf. B: Biointerfaces*, **2016**, 142, 141-147
9. A. Matilainen, M. Vepsäläinen, M. Sillanpää, Natural organic matter removal by coagulation during drinking water treatment: a review, *Adv. Colloid Interf. Sci.*, **2010**, 159, 189-197
10. Rahimi, B.; Jafari, N.; Abdolahnejad, A.; Farrokhzadeh, H.; Ebrahimi, A., Application of efficient photocatalytic process using a novel BiVO/TiO_2-NaY zeolite composite for removal of acid orange 10 dye in aqueous solutions: Modeling by response surface methodology (RSM). *Journal of Environmental Chemical Engineering* **2019,** *7* (4).
11. Amorim, R.; Vilaça, N.; Martinho, O.; Reis, R. M.; Sardo, M.; Rocha, J.; Fonseca, A. M.; Baltazar, F.; Neves, I. C., Zeolite Structures Loading with an Anticancer Compound as Drug Delivery Systems. *The Journal of Physical Chemistry C* **2012,** *116* (48), 25642-25650.
12. Motazedi, K.; Mahinpey, N.; Karami, D., Preparation and Application of Faujasite-Type Y Zeolite-based Catalysts for Coal Pyrolysis using Sodium Silicate Solution and Colloidal Silica as Silicon Source. *Chemical Engineering Communications* **2015**, 203 (3), 300-317.
13. V. Valtchev, S. Mintova, Layer-by-layer preparation of zeolite coatings of nanosized crystals, *Micropor. Mesopor. Mater.* **2001**, 43, 41–49.
14. D.M. Ginter, A.T. Bell, C.J. Radke, The effects of gel aging on the synthesis of NaY zeolite from colloidal silica, *Zeolites*,**1992**, 12, 742-749.
15. W. Bo, M. Hongzhu, Factors affecting the synthesis of microsized NaY zeolite, *Micropor. Mesopor. Mater*. **1998**, 25, 131–136.
16. H. Kacirek, H. Lechert, Rates of Crystallization and a Model for the Growth of NaY Zeolites *J. Phys. Chem*. **1976**, 80, 1291.
17. Zhu, D.; Wang, L.; Fan, D.; Yan, N.; Huang, S.; Xu, S.; Guo, P.; Yang, M.; Zhang, J.; Tian, P.; Liu, Z., A Bottom-Up Strategy for the Synthesis of Highly Siliceous Faujasite-Type Zeolite. *Adv Mater* **2020**, 32 (26), e2000272.
18. M.E. Davis and R.F. Lobo, Zeolite and Molecular Sieve Synthesis, *Chem. Mater.*, **1992**, 4, 756-768.

19. Azizi, S. N.; Alavi Daghigh, A.; Abrishamkar, M., Phase Transformation of Zeolite P to Y and Analcime Zeolites due to Changing the Time and Temperature. *Journal of Spectroscopy* **2013**, 2013, 1-5.
20. 1.Gross-Lorgouilloux, M.; Caullet, P.; Soulard, M.; Patarin, J.; Moleiro, E.; Saude, I., Conversion of coal fly ashes into faujasite under soft temperature and pressure conditions. Mechanisms of crystallisation. *Microporous and Mesoporous Materials* **2010**, 131 (1-3), 407-417.
21. M Aimen Isa *et al*, Zeolite NaY Synthesis by using Sodium Silicate and Colloidal Silica as Silica Source, *IOP Conf. Ser.: Mater. Sci. Eng.* **2018**, 458, 012001
22. Prabir K. Dutta and Josip Bronic, Mechanism of zeolite formation: Seed-gel interaction, *ZEOLITES*, **1994**, 14, April/May
23. Edelman, R.D., Kudalkar, D.V., Ong, T., Warzywoda, J. and Thompson, R.W. Crystallization phenomena in seeded zeolite syntheses, *Zeolites* **1989**, 9, 496-502
24. Tsokanis, E.A. and Thompson, R.W. Further investigations of nucleation by initial breeding in the Al-free NH_4-ZSM-5 system *Zeolites* **1992**, 12, 369-373
25. H. Kacirek, H. Lechert Rates of Crystallization and a Model for the Growth of NaY Zeolites *J. Phys. Chem.*, 1967, 80, 1291-1296
26. Mohd Nazir, L. S.; Yeong, Y. F.; Chew, T. L., Controlled growth of Faujasite zeolite with NaX topology by manipulating solution aging and Na_2O/Al_2O_3 ratios. *Colloids and Surfaces A: Physicochemical and Engineering Aspects* **2020**, 600.

Chapter 2 Zeolite NaY water absorption properties and behaviors

2.1 Introduction

Water adsorption, or alternatively, dehydration is a common and crucial process in daily life and numerous industrial fields. For instance, in pharmaceutical industries, dehydration technology has a significant impact during manufacture process as it can remove water from the medicine thus promote stability and prolong the shelf life for some valued proteins and antibiotics.[1] Vapor removal is also an essential step in natural gas purif1ication in energy industries.[2] More generally, the primary reason of the perishability of fruits and vegetables is the high-water content, a variety of desiccants have been explored and used for food preservation. Therefore, the research on dehydration materials is required to meet industrial demand and to conserve energy and economic cost.

Zeolite ("molecular sieve", in other words), silica gel, and clay mineral are traditional commonly used desiccant in industries and heat pump/cooling systems. Silica gel, the granular porous silicon dioxide made from sodium silicate, is the most widely used desiccants in everyday life. It works like the sponge, which can absorb water into internal pores. It has an excellent capacity to absorb about 35-40 % water weight of its own dry mass.[3] It can desorb the trapped water when heated to 82 ℃. However, the water adsorption ability is poor under low relative humidity (RH), and it will lose some of its dehydration capacity. The water uptake of silica gel can decrease drastically as temperature increases, as shown in the Figure 2.1.[32] A more detailed comparison of the common desiccants is listed in Table 2.1.[4] Due to the original difference in the chemical structures, which zeolites have special sized channels, pores and cages, other absorbents do not have size selectivity and have lower absorption speed, and all of them have some drawbacks when then relative humidity and temperature varies except zeolite. Moreover, in Figure 2.2,[5] desiccants water

absorption capacity under relative vapor pressure has been investigated. The amount of water absorbed is plotted for various absorbents as the relative vapor pressure p/p^0 increased. Zeolites and silica gel shows initial parts of the isothermal shapes which are consistent with Henry's law, though silica gel exhibits a much lower Henry's law K constant, indicating the poor adsorption ability at lower relative vapor pressure. The lack of selectivity and poor adsorption capacities at some cases make silica gel and clay to be less preferable for lots of industry process. Whereas, in general, the interaction of water's persistent and large dipole moment with a zeolite cation causes the extremely high and fast water adsorption on zeolites,[5] which make zeolite behaves steep uptake of water in isothermal graphs and it becomes one of the most efficient and popular traditional desiccants for practical use.

Table 2.1. Properties comparison of different type of absorbents[4]

Property	Molecular Sieve	Silica Gel	Montmorillonite Clay	CaO	Ca_SO_4
Adsorptive Capacity at low H_2O Concentrations	Excellent	Poor	Fair	Excellent	Good
Rate of Adsorption	Excellent	Good	Good	Poor	Good
Capacity for Water at 77°F, 40% RH	High	High	Medium	High	Low
Separation by Molecular Sizes	Yes	No	No	No	No
Adsorptive Capacity at Elevated Temperatures	Excellent	Poor	Poor	Good	Good

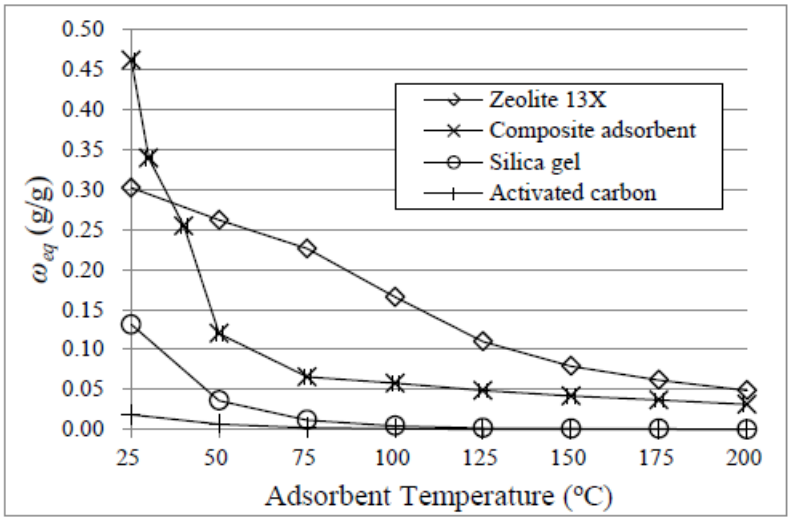

Figure 2.1. Equilibrium H_2O uptake capacity of different desiccants (zeolite, silica gel, activated carbon, composite) by temperature.[32] Reproduced with permission.

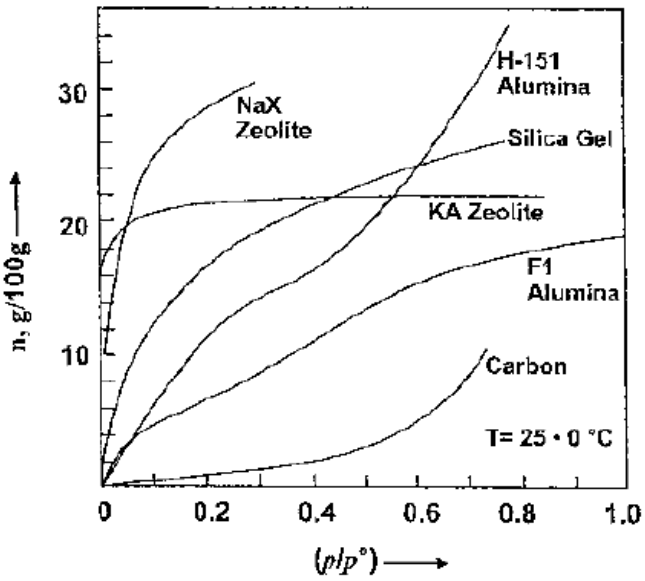

Figure 2.2. Adsorption isotherm graph of H_2O vapor on various desiccants at 25 °C. p/p^0 is the relative vapor pressure. [5] Reproduced with permission from Sircar.

Besides, there are various novel absorbents that have been explored for water absorption. Metal–organic frameworks (MOFs) have been studied and developed in recent years because of the possible applications especially in gas separation and adsorption areas. For instance, new zirconium MOFs, MOF-801-P and MOF-841[6] exhibit promising water absorption abilities and can be designed and applied in thermal batteries and more specially, MOF-841 can be used to catch and release ambient water in the air in secluded desert areas. MIL-100(Fe),[7] another one of the most famous MOFs, synthesized dry gel conversion, shows the water moisture adsorption ability of 0.75 g/g and promising desorption capacity compared to traditional zeolites. Moreover, synthesized pure double-walled carbon nanotube[8] can adsorb water molecules via its interstitial and interbundle nanopores. Novel hygroscopic materials, for example, LiCl, $MgCl_2$, and $CaCl_2$ with deliquescent liquid sorbents have impressive water absorption capacity.[9] Even so, almost all the above-mentioned innovational absorbents are at the stage of laboratory research, some of the techniques are not mature enough for practical use. Additionally, the particularity of the water adsorption capacity limits the possibility of being applied for wide applications and techniques. And it is noted that the high energy and economy cost for desorption and regeneration of the material is one of the fundamental challenges of the new absorbents,[9] especially for some materials that have poor hydrothermal stability. The future investigation and optimization of novel absorbents is promising but it is still a long way before applied into practical manufacturing. Taking all the factors into consideration, zeolites become a powerful competitor in all the absorbents, since they have the steep water uptake even at relative low humidity and can stay its structure integrity, and have low economic cost to be synthesized, manufactured, and regenerated.

During recent decades, lots of efforts have been devoted to evaluating and promoting the water adsorption capacities of multiple type of zeolites. In general, the adsorption ability is defined using the equation below.

$$Water\ absorption\ capacity\ = \frac{Mass\ of\ water\ adsorbed}{Mass\ of\ absorbent}$$

The water adsorption upper limits of various zeolites and their ion-exchanged forms have been explored. Gismondine (GIS) type zeolite, or so-called P zeolites, have the same framework and pores structures though the Si/Al could be different.[11] It has the most amazing water absorption capability among all the studied zeolites. For P7 zeolite[12] with the Si/Al ratio of 2.11, the maximum water amount it can adsorb is 1.39 g/g. P6 zeolite[12] with Si/Al ratio of 2.34 has capacity of 1.30 g/g, P4 is 0.97 g/g and P5 is 0.64 g/g. Given the fact that one of the most commonly used laboratories desiccant 4A zeolite,[12] has the water adsorption capacity of 0.25 g/g, P type zeolites upper limit is more than 5-fold larger compared to 4A zeolite. NaA has the water adsorption capability of 0.29 g/g, [13] 13X and LTA_{SS} have the value of 0.26 g/g, [14] Faujasite NaY has the value of 0.33 g/g,[14] yet all of them are much weaker than the P type of zeolites based on the numbers. However, the main drawback of P type of zeolite is the poor water uptake at relative low pressure as shown in Figure 2.3.[14] Compared with Faujasite and LTA zeolites which are highly hydrophilic,[15] synthesized P type zeolites exhibit the poor hydrophilicity characteristics of their structures though the maximum uptake is surprising high. According to the existing feature that restrict the practical use of P type zeolites, it is not wise to generalize the use of P zeolites for non-ideal efficiency and unpracticality. Among all the discussed various zeolites, NaY with 0.33 g/g water adsorption capacity becomes an ideal desiccant.

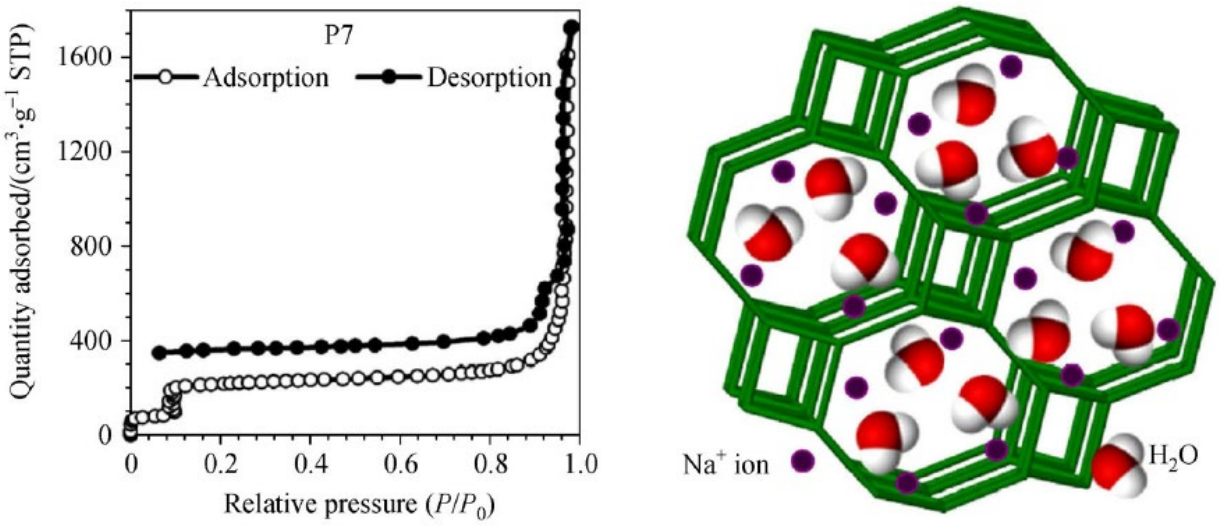

Figure 2.3. Water adsorption and desorption isotherm graph of P7 zeolite, and its framework. [14] Reproduced with permission from Wang and LeVan.

The hydrophilicity of zeolites mainly relies on the Si/Al ratio of the framework, structure type and extra-framework cations produced by ion exchange. It has been reported that steam treatment or acid/base chemical method[16] can lead to the dealumination of zeolite, which gives rise to a higher Si/Al ratio by pulling out Al from the tetrahedral framework and leaving over cavities. The dealuminated Y zeolite, according to studies, has less strong adsorption sites and weaker hydrophilic properties.[17] Thus, it is unnecessary to modify and reduce the Si/Al ratio of the framework. Mo¨ıse et al. explored the water vapor adsorption capacities on barium exchanged Faujasite zeolites (BaX and BaY) using thermogravimetry and calorimetry method given isothermal or isobaric conditions.[18] The Ba exchanged Y zeolites exhibit a better water adsorption affinity comparing to NaY type zeolite. Though the overall water adsorption capacities and the reusability of BaY is still weaker than NaY zeolite. Moreover, the ion-exchange process will increase the basis cost of producing Y type zeolites. Given the fact that the inexpensive commercial NaY has been used for industrial process in recent decades mainly in petroleum refining, catalytic

reactions and gas separations, the investigation and optimization of NaY water adsorption capacities can contribute to the desiccant field and the engineered material can be employed for industrial dehumidification technique and manufacturing.

Besides, dehydration of hydrated zeolites is one of the essential steps in industrial desiccation process. The dehydration is the sustainable utilization of zeolite materials, and sustainability will put the positive effect on economy, ecology, and energy conservation. Given the fact that estimated 98,000 tons of natural zeolites were produced in the United States for one year, which rose more than sixfold in recent three decades,[21] the reuse and recycle of zeolites is the topic worthy of study. The volumetric and structural impacts of heating zeolites were separated into three general groups by Alberti and Vezzalini.[27] The first type has the reversible dehydration property with little or no modification of the framework or unit-cell volume, in some cases accompanied by rearrangement of extra framework cations and residual water molecules; second is complete or almost complete invertible dehydration with a huge distortion of the framework and a significant decrease in unit-cell volume; last one has the reversible dehydration property at low temperature, usually accompanied by significant modifications of the framework, followed by irreversible changes owing to T-O-T (tetrahedral cation-oxygen-tetrahedral cation) breaking. For Faujasite zeolite, which has good thermal stability, won't be collapse until reaching 800 ℃, the temperature can be fluctuate based on the Si/Al ratio. Rare earth introduced NaY has the collapse temperature reach up to nearly 1000 ℃.[28] Thus, heating under temperature from 100 ℃ to 800 ℃ is the most common and traditional way to dehydrate zeolites in industries and labs. However, the desorption of zeolites usually achieved through two steps, first is for the water molecules condensed in the channels and pores and be physically adsorbed on the surface, they would be removed first, then chemically bounded water would be removed later. Hot air, at these low temperatures, only interact with the

surface layer of the zeolite, making it less efficient to remove water. If the temperature is not high enough, for instance, the recent study shows chemically bonded water cannot be removed from SOD type of zeolite unless reach the temperature of 190 ℃.[29] Only when after enough heating can the temperature reach close to 200 °C, at which most water can be desorbed, and diffusion is easy in zeolites, making dehydration a quick process. At this temperature, even the most tightly bound water to Na in sodalite cages can be desorbed, though flowing vacuum or dehumidified air may need to be applied to avoid re-adsorption of water when cooling down the zeolite. In this way, it's not quite worth to consume a large amount of energy and time to recycle and dehydrate the used zeolite on account of the low manufacture cost of zeolite synthesis. However, in recent years, microwave has become an alternative way of traditional heating. Microwave assisted dehydration has become one preferable tool to get the reusable materials though there's not enough study based on drying zeolite. Various types of ceramics and other inorganic compounds, including zeolite, can be heated by the household microwave (2.45 GHz) oven.[30] It has been proposed that the main mechanism of microwave heating is owing to dipole orientation and ionic conduction, adsorbed water plays a crucial function in preheating the zeolite during the early stage of microwave dehydration and zeolite won't be "activated" without water inside the framework.[31] Here, the dehydration patterns of commercial zeolite NaY have been measured using hot nitrogen heating and microwave heating for comparison.

In Figure 2.4, it shows the schematic drawing of a zeolite particle of the commercial zeolite beads, the gas molecule transport route during the adsorption or desorption process is represented as well.[19] The binder material such as clay can occupy 10–20 wt. % by the pellet mass, which cause the lower water adsorption efficiency and block some of the pores and channels of zeolites. To evaluate and promote the water adsorption behavior of Faujasite Y, the commercial Y type zeolites

and as-synthesized NaY water adsorption capacities were tested and compared, ^{1}H solid-state NMR spectra were measured to examine and explain the relationship of water content change and different bonding in the framework. Furthermore, the hydration and dehydration pattern of bulk zeolite samples were determined by neutron image. The dehydration or dehumidification of the commercial and lab-made Y zeolites were also explored.

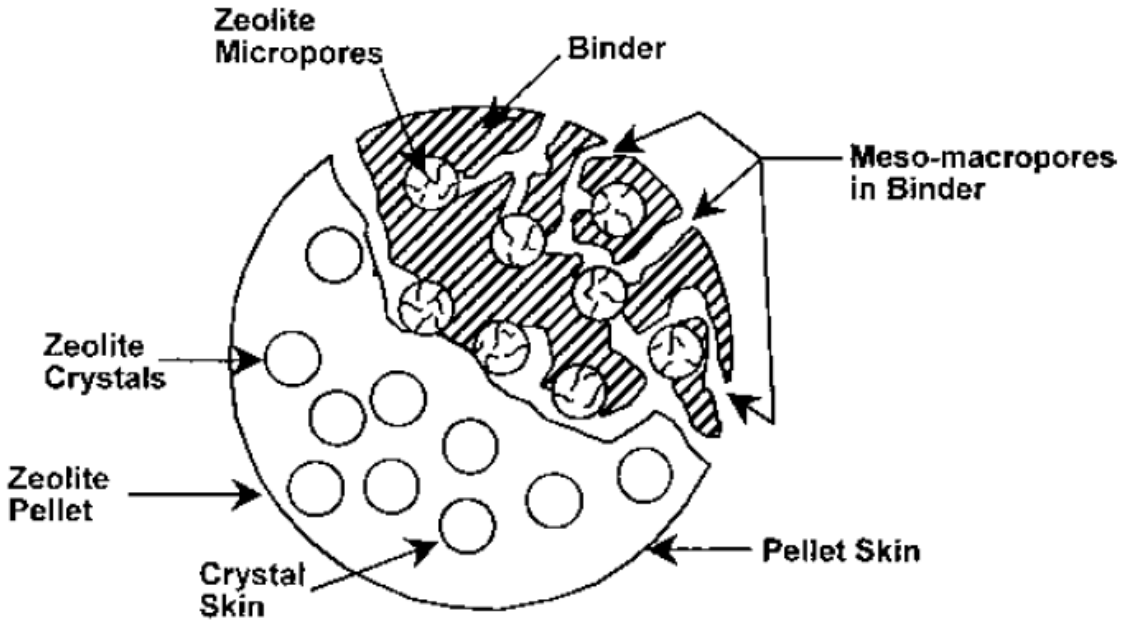

Figure 2.4. Schematic drawing of one zeolite bead with binder inside. [19] Reproduced with permission from S. M. Auerbach.

2.2 Experimental

2.2.1 Materials and methods

NaY zeolite with Si/Al ratio of 1.69 was synthesized as stated in the previous part. Commercial NaY pellets Na-Y-Pe were purchased from ACS Material, LLC. The diameter of the pellet is around 2~3 mm, with the unit cell size of 2.465-2.472 nm, the average size of the particle is <6 μm. NaY pellets samples were also grinded for >2 hours manually using mortar and pestle to be

compared with synthesized NaY powder. The morphologies of NaY pellets and pellet powder were shown in Figure 2.16.

Dry zeolite samples were obtained by heating in the furnace under >200 ℃ overnight. For the subsequent water adsorption test, room temperature deionized water in the petri dish was used the water vapor source. Zeolite samples were put into the weighing boat or scintillation vial. The hygrometer was placed in between the petri dish and samples. The humidity was monitored by the hygrometer, for the water vapor adsorption in this experiment, the humidity is controlled at 98-100 % relative humidity under 25.0 -25.3 ℃. The schematic drawing of the water adsorption test was shown in Figure 2.5. Mass change of zeolite samples were measured using microbalance. All the tests were repeated for the consistency. For water desorption measurement using hot air and microwave, the setup is showed in Figure 2.16.

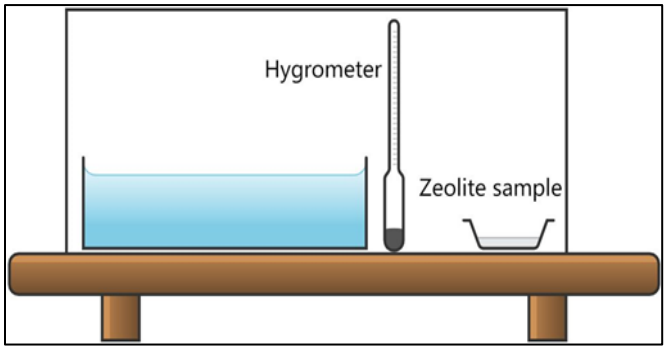

Figure 2.5. Schematic diagram of water adsorption test setup. A rubber sheet is placed under the inverted tank to ensure the air tightness.

Synthesized NaY zeolite samples were dried in the furnace >200 ℃ overnight first, then put into the aluminum containers with PTFE caps and prepared for various dehydration and hydration levels for the neutron images.

2.2.2 Characterization

X-ray powder diffraction (XRD, Bruker D8 Eco) of the grinded commercial NaY pellets powder and synthesized samples were obtained using Powder X-ray diffractometer with Cu Kα radiation (λ = 1.5418 Å) operated at 40 kV and 25 mA. The samples were mounted on a zero-background holder and diffraction patterns were scanned over the range of 2-50 ° in 2θ scale with a step size increment of 0.02°. Scanning electron microscopy (SEM, FEI Scios 2 DualBeam) images were acquired by Dr. Lien. Samples were prepared in lab, and neutron images were taken at The McClellan Nuclear Research Center (Sacramento, the United States) by Dr. Wesley Frey and his co-workers. The contrast was adjusted to reveal the water penetration and diffusion. ^{1}H solid-state nuclear magnetic resonance spectroscopy (ssNMR, Bruker, 500 MHz Avance Solids NMR) was used to characterize the structural interactions of water molecules bond to synthesized NaY zeolite samples. Theoretical ^{1}H solid-state NMR calculations and simulations were done by our collaborator Donadio's lab.

2.3 Results and discussion

To confirm the reliability of the comparison between synthesized NaY and commercial NaY pellets, Y pellets were grinded to fine powder as stated. Figure 2.6 shows the XRD pattern of Y pellet powder, which is consistent with synthesized NaY. The differences in the baseline and some of the peaks mainly due to the presence of the binder in commercial Y zeolite, which possibly could be one or several types of clay. Figure 2.7 represents the SEM morphologies of grinded NaY pellets.

In order to eliminate the effects of different sample morphologies, first, the water adsorption abilities were examined using 1.0 g of Y pellet and pellet powder under p/p^0 =1.0 under room temperature 25.0 -25.3 ℃, as shown in Figure 2.8 (left). The trend and the water adsorption rate

performed almost the same, and it reached the plateau and the water adsorption weight percent kept constant after 120 h.

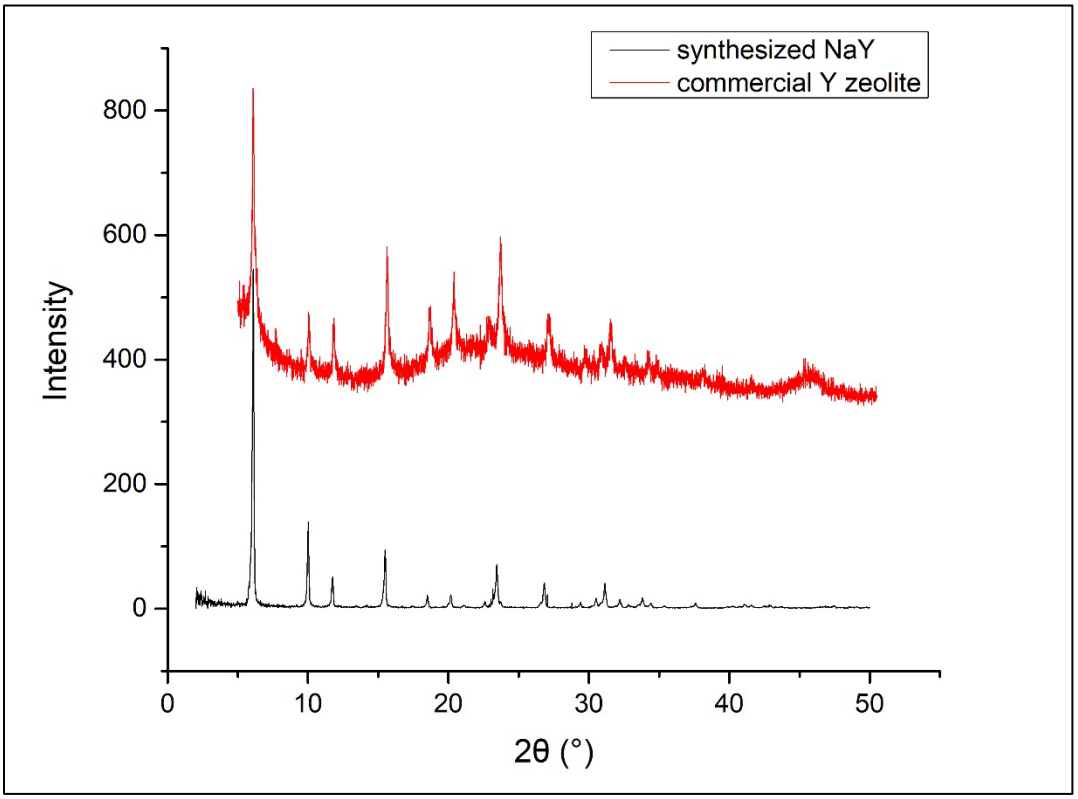

Figure 2.6. Powder X-ray diffraction patterns of dried commercial Na-Y-Pe powder (top) and synthesized NaY zeolite powder (bottom).

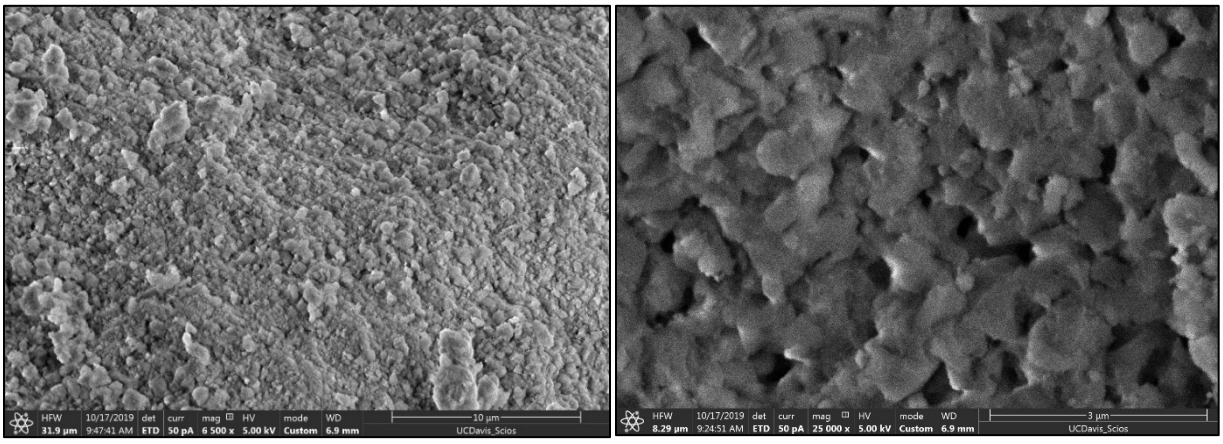

Figure 2.7. SEM images of grinded commercial NaY pellets powder.

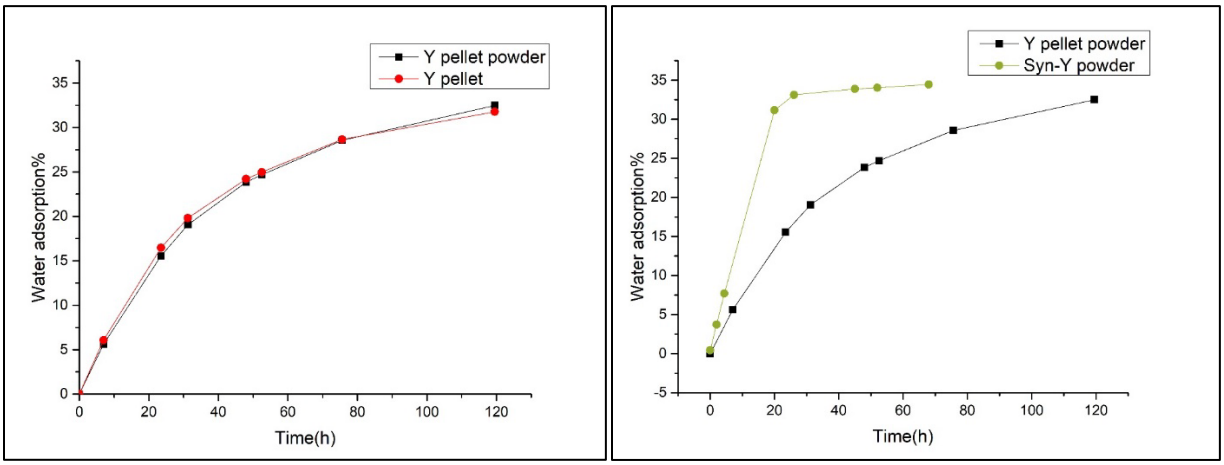

Figure 2.8. Water vapor adsorption curves under p/p^0 =1.0 and 298 K. Left: 1.2 g of NaY pellets and NaY pellets powder, which shows similar adsorption rate and trend. Right: 1.2 g of NaY pellets powder and synthesized NaY powder, syn-Y powder shows a steeper adsorption rate.

Then, 1.2 g of commercial Y powder and lab-made 1.0 g NaY samples were also evaluated in Figure 2.8 (right). The much milder adsorption rate can ascribe to the much large particle size of commercial NaY (avg <6 μm) compared to the sized of synthesized particles (avg ≈ 350 nm) and the existence of binders which is assumed 10 ~20 wt.% of the whole mass of pellets which can block the vapor transfer. The higher silicone to aluminum ratio of Y pellet which is > 2.5 and the slightly lower crystallinity >88% may also cause the less steep adsorption rate. Meanwhile, the upper limit, in other words, the maximum water vapor adsorption capacity of two tested samples is same. The largest percent weight of water absorbed for commercial sample is 32.5 ~ 33.5% and for synthesized sample is 34.5 ~ 35.5%. The numbers obtained were in agreement with the literature value of NaY which is 0.33 g/g.[14]

The thickness of the sample loaded in the container may also affect the water vapor transfer. To prove it, 0.5, 1.0, and 2.5 g of dried zeolite was prepared and loaded in 20 mL scintillation vials

and used for water vapor adsorption test under p/p^0 =1.0 at room temperature. As shown in Figure 2.9, 0.5 g and 1.0 g of synthesized NaY sample have similar trend, and both of them reach the plateau of 34.5 ~35.5% maximum water uptake after 27 hours. However, for 2.5 g sample loaded in the sample container with larger sample thickness, it shows a less steep water uptake rate. The rate difference meets the expectation; for bulk sample with thinner thickness, there are spaces and cavities in the powder by which water vapor can pass through can diffuse; for thick bulk sample, the bottom layers desiccant cannot contact outside water vapor easily so that reduce the adsorption speed. Nevertheless, the overall water uptake capacities are the same, the blue curve in the Figure suggests it can reach the almost the same maximum adsorption percentage 34.53% but after 102 hours. On the other hand, previous studies proved that maximum water uptake of zeolites would decrease as the relative humidity decreases.[20]

The above water adsorption kinetics of various amount zeolites provokes the consideration that when the situation converted to micro-level, for instance, the water adsorption rate of 10 μm thickness of zeolite should be much larger than the bulk samples which have the thickness > 0.5 cm. And this assumption is based on the manner that water molecules diffuse into the desiccants from contact surface into interior layers. It has been studied that water movement is primarily driven by capillary absorption and diffusion, the diffusion which also called osmosis is the main way water pass through the desiccants. The growth in entropy produced by the movement of free water molecules is the driving power of water diffusing in hydrophilic zeolites. The process that dried zeolite being hydrated and saturated is supposed to be started with the top layer then water molecules will transfer to deeper layers of zeolite particles. There could be two possible patterns that water molecules gradually saturating the zeolite particles, one is water saturate the top layers of dried zeolite particle first, then go to the subsequent lower layers, the bottom layer would be

saturated in the end; the other way is water molecules pass through all the layers of particles until reach the bottom layer and saturate from the bottom to the top, and the top layer would be the last saturated layer. The investigation of the saturation pattern and dehydration of molecules in zeolite can improve the using efficiency and minimizing the waste of zeolites as desiccant in many areas. Neutron imaging has been used to reveal the internal plant water dynamics[21] and to observe the adsorption of water by commercial zeolite 13X beads.[22] X-ray imaging is not applicable in this case because hydrogen is almost invisible to the x-rays while neutron cross section of hydrogen is much larger. To monitor the water diffusion process without using the embedded hygrometer that may impact the motions of water molecules, neutron imaging was used as the tool in this experiment to exhibit the real picture of zeolites with different levels of hydration as shown in Figure 2.10 and Table 2.2. Neutrons have a relative weak interaction with varied materials, in this experiment, the aluminum sample containers were designed so that the strong neutron beam can directly penetrate the container walls and still sensitive to the water inside the container. The dehydrated NaY samples were put into the container and hydrated to different level then capped with compact PTFE caps to avoid further hydration or dehydration. In Figure 2.10, after calibration of the background and increase the contrast, the dynamic of water molecules diffusion is represented. Sample #1 and #2 were hydrated under ambient environment (RH 33%) for 4 days and 2 days. Sample #3 and #4 were hydrated under relative humidity 66% for 4 days and 2 days. Given the fact the brighter area means higher water content in the neutron images, the top layers of all the 4 samples are hydrated first, then water molecules moved down gradually, and it wouldn't hydrate the next layer until above layer is fully hydrated, which is consistent with the first type diffusion type we proposed. It is obvious in sample #5 and #6 as well, which is fully hydrated and hydrated to 9.7% under RH 100%. And according to the integrated densities in Table 2.2, sample

#5 has the highest density which corresponding to the highest hydration level. Samples #7 and 8 are fully hydrated samples dried at 100 °C for 20 and 40 min. Uniform water distribution is observed in these two samples, especially in #8 when the image is not saturated, which indicates the desorption under heat is intense and uniform, there's no spatial difference for desorption process of the water molecules. The investigation of adsorption and desorption pattern help to understand the motion of water molecules and can be utilized to improve the technological design in industries.

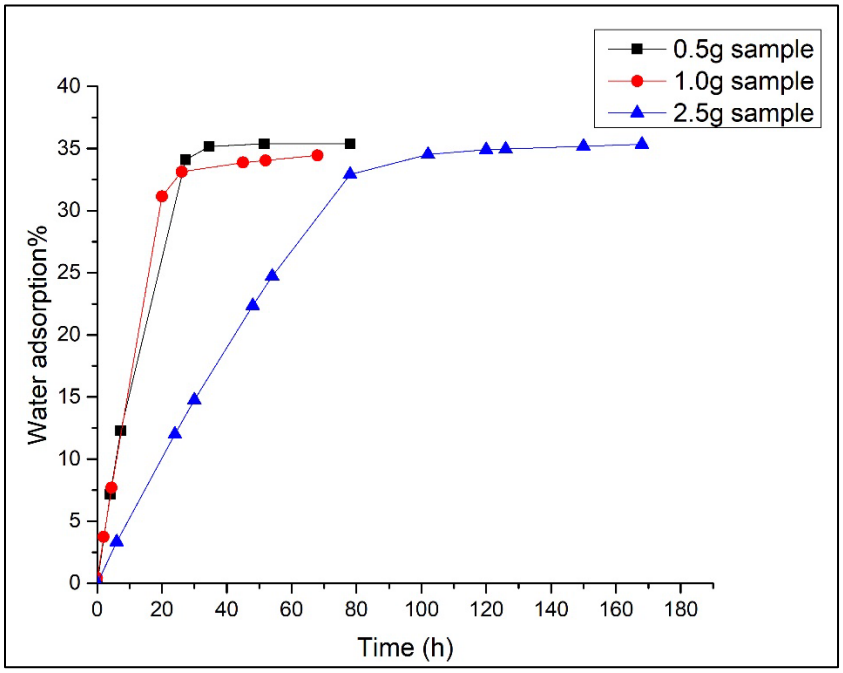

Figure 2.9. Kinetics of water vapor adsorption curves of dried synthesized NaY samples under p/p^0 =1.0 at 298 K. Black: 0.5 g of NaY sample, reach plateau at around 27 h. Middle: 1.0 g of NaY sample, reach plateau at around 27 h. Right: 2.5 g of NaY of NaY sample, reach plateau at around 102 h.

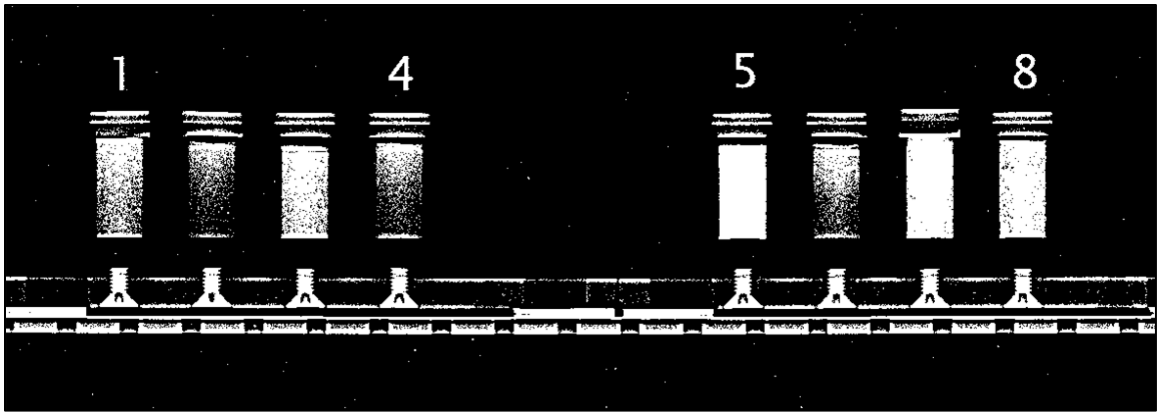

Figure 2.10. Neutron imaging of hydration of zeolites in aluminum containers. Brighter areas mean high water content in the sample. Totally eight samples were imaged, 1 - 8 from left to right. Samples #2, 4 and 6 are hydrated zeolites from fully dehydrated zeolites filled in the aluminum cylinders with PTFE caps.

Table 2.2 Neutron imaging of various hydration and dehydration levels of NaY zeolites.

	Area	Mean	Max	Integrated Density
1	6148	40.554	91	249325
2	6148	41.512	83	255214
3	6148	47.061	130	289333
4	6148	40.109	75	246593
5	6148	62.947	172	387000
6	6148	40.027	81	246084
7	6148	54.019	148	332106
8	6148	52.136	125	320531

Besides, the interior mechanism of adsorption and desorption, to be specific, which sites water molecules are situated is another essential question. Nuclear magnetic resonance (NMR)

spectroscopy is one primary way in the study of solids, and the solid-state NMR has been used as a modern experimental method to characterize the structures of zeolites.[23] The chemical shift caused by the interaction of the nuclear spin with the magnetic fields induced by the electronic environment can offer the evidence of chemical interactions or bonding in the zeolite structures. From previous studies, ^{29}Si magic angle spinning (MAS) NMR spectra can be used to calculated Si/Al ratio of the zeolite framework and the distribution of Si and Al can be determined, ^{13}C MAS NMR can be used to identify interactions between organic molecules and zeolite.[24] Moreover, ^{1}H one-dimensional (1D) solid-state NMR spectra were examined for different dehydrated levels of Kanemite,[25] also been measured for the investigation of benzene adsorption on dried NaY zeolite.[26] Figure 2.12 shows the ^{1}H MAS NMR spectra of zeolite NaY with different hydration/dehydration levels. For the blue curve, which is the hydrated NaY, has the peak at downfield and has the highest intensity. Generally, hydrogen bonds exhibit a downfield chemical shift since the electrostatic polarization caused by the de-shielding of protons. Here, adsorption of H_2O molecules demonstrates that the peak at 4.7 ppm originated from the Brønsted acid sites of the zeolite framework. The chemical shift for mildly dehydrated sample (100 ℃) and regular dehydrated sample (250 ℃) is 4.0 ppm and 1.8 ppm, also the intensities are much lower. The chemical shifts exhibited are much lower than the literature values of H-ZSM-5,[24] which is consistent with their higher acidity. Theoretical simulations (Table 2.3) were done by our collaborators, using Gauge-Including Projector Augmented-Wave method and Gaussian and Augmented Plane Wave Method. When Al content is constant, 29% was used for the calculations, as number of water molecules accommodated in the framework increases, the chemical shift increases. The trend that more water adsorption in the zeolite framework causes the downfield shift has been revealed in both experimental data and theoretical data. Moreover, NMR data can be used to identify binding sites

in zeolites that interact with water molecules and there are generally three types of sites. As shown in Figure 2.11 and Figure 2.12, the strongest interactions are between water molecules and sodium ions in the sodalite cages, which is 1.8 ppm in the experimental data and manifested by the peak at 2.0 ppm in the simulation results. The medium interactions are between water and aluminum sites or between water and oxygen next to aluminum sites, as indicates at the peak 4.0 ppm. This conclusion is confirmed by energetic theoretical simulations in Figure 2.13, which shows the binding energy of water in zeolites is higher when more aluminum is added. The most fragile interactions are between water and silicon sites or between water and oxygen next to silicon, as shown by the peak at 4.7 ppm. The interactions found out are the mechanism basis for NaY water adsorption and desorption technique.

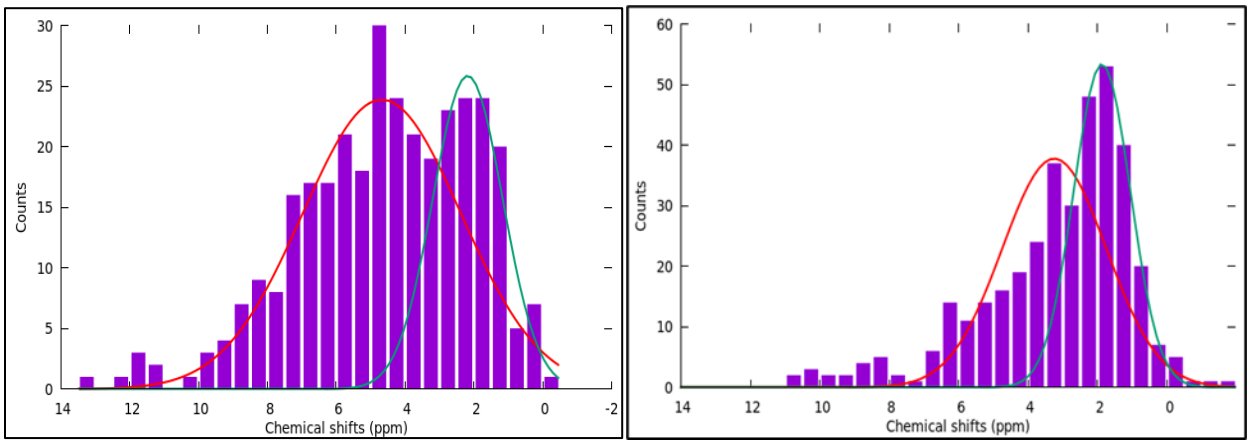

Figure 2.11. Theoretical simulation of ^{1}H MAS NMR results for different amount of water molecules in NaY framework under 303 K (left) and 473 K (right).

Table 2.3. Theoretical calculations of chemical shift and adsorbed energy change for different number of water molecules in the framework.

Number of H_2O	Ads. Energy (KJ/mol) (Sodalite-cage, [Al]= 29%, 14 Al, 14 Na)	Chemical Shifts (ppm)
1	-100.58 ±13.67	4.57 ± 1.92
2	-87.74 ± 3.93	5.17 ± 1.03
3	-87.21 ± 7.01	5.46 ± 0.64
4	-84.89 ± 6.78	6.30 ± 0.34
5	-67.93 ± 12.27	7.52 ± 0.38

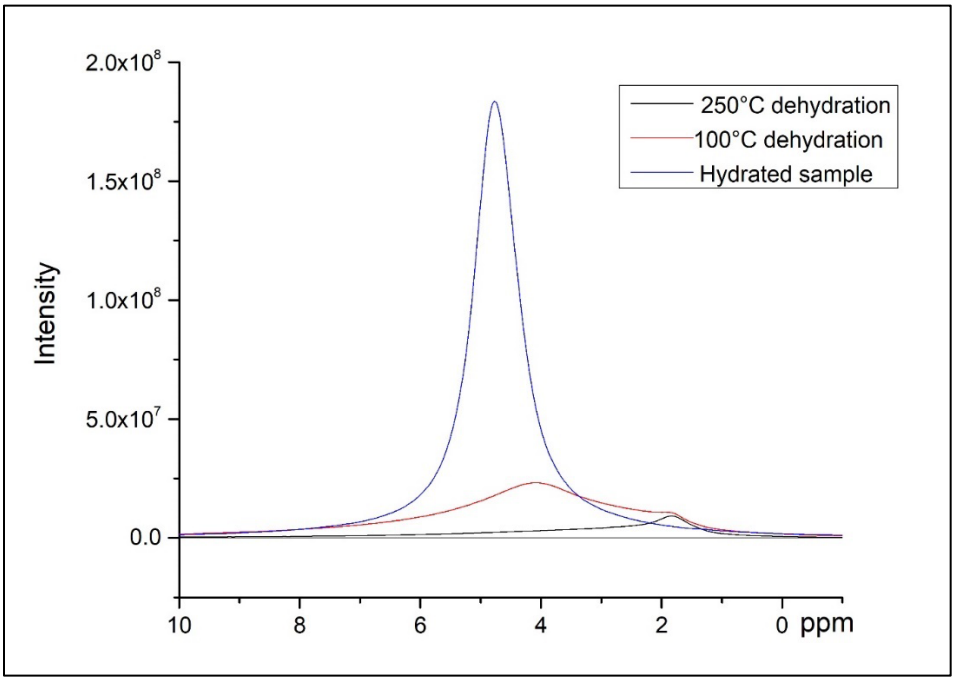

Figure 2.12. ^{1}H MAS NMR of synthesized zeolite NaY with different hydration/dehydration levels. Red: sample is prepared by dehydration under 373 K.

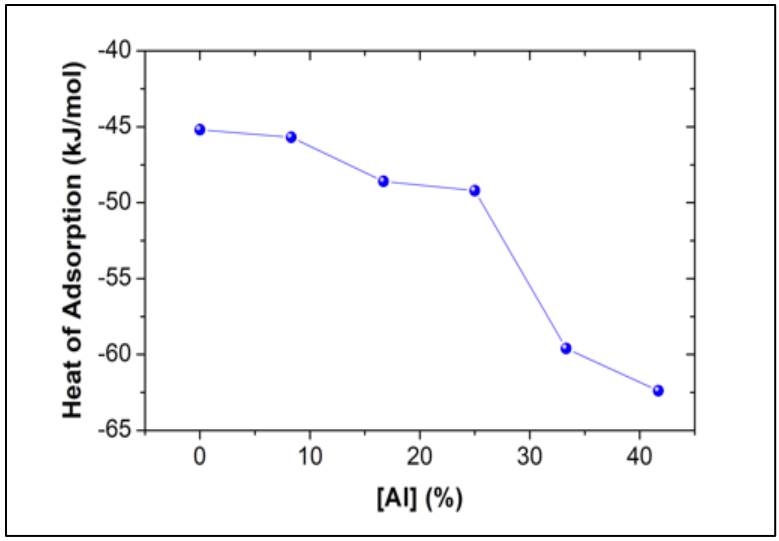

Figure 2.13. Binding energy or heat of formation of the water-Faujasite system as a function of Al (in atomic %). The heat of formation increases by around 40% as 40% of Al is added into the zeolite framework.

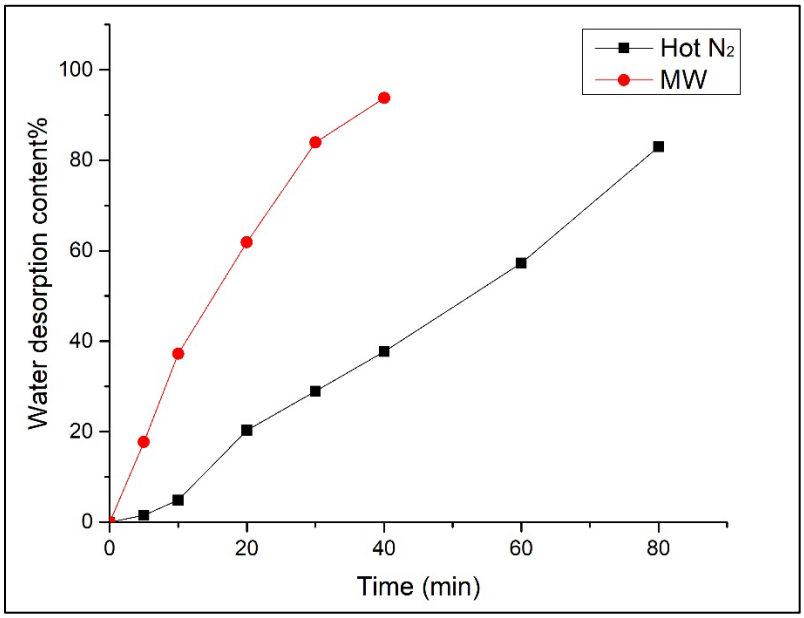

Figure 2.14. Comparison of dehydration of fully hydrated commercial millimeter-sized zeolite particles by hot N_2 (black) and microwaves (red). Hot N_2 is heat by electricity. Both the hot N_2 and microwave device are powered by 250-350 W 110 V AC.

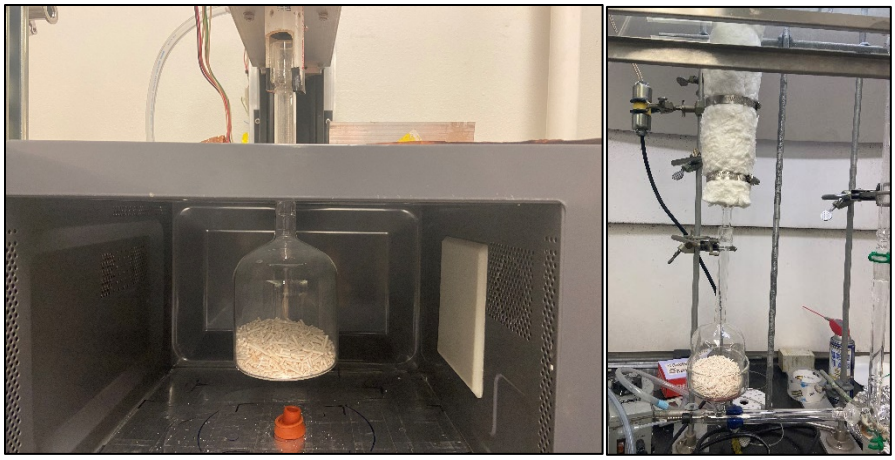

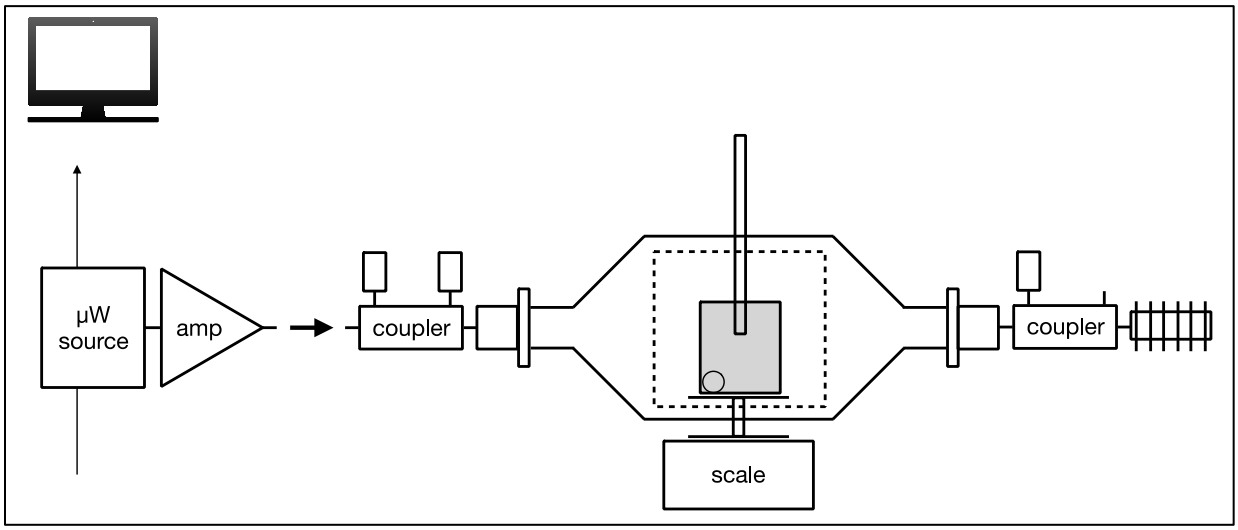

Figure 2.15. Pictures and schematic diagram of the apparatuses. The top-left shows the microwave heating chamber in the microwave oven and the top-right the hot air device. The sample chamber is the same, which is a home-made glassware with laser-drilled holes at the bottom to allow air flow through. The microwave device is a modified commercial microwave reactor, and the hot air device is a home-made device with a heating element. The hot air reactor is thermally insulated. The bottom panel shows the improved microwave device used to study microwave drying of zeolites. The samples are places in an identical glass container in the cavity shown here (right above the scale).

Figure 2.16. The picture of morphologies of grinded commercial NaY pellets powder and NaY pellets.

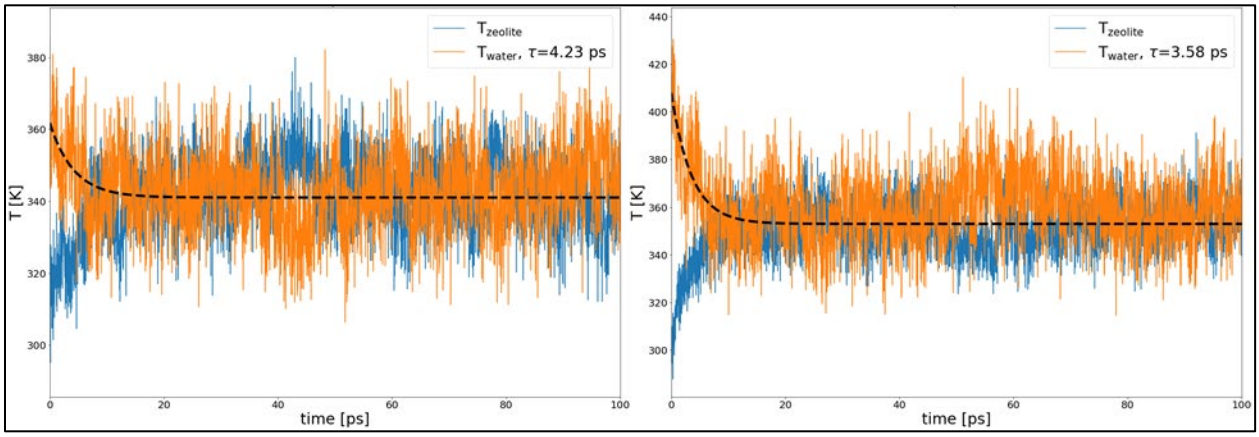

Figure 2.17. Quantum chemistry simulation of energized (left 360 K, right 440 K) water in zeolites. The results suggest that energized water passes its energy to the zeolite host within picoseconds, which implies that zeolites heat up quickly by the absorbed water.

To corroborate and evaluate the assumption that the more efficient way to dehumidify the zeolite is using microwave heating, two setups were designed and built as displayed in Figure 2.16. For a 5-min drying, microwave heating is over 11.6-fold as efficient as hot N_2 drying. When the heating times are long enough, the difference between the two decreases. At 30 min, the difference is still 3-fold. Based on the reality that fully dehydrated zeolite is not necessary for industrial use, zeolite that dehydrated >90% can be good for most of the drying technologies and other applications,

microwave is at least 3-fold efficient than hot N_2, which reveals the powerful potential of fast microwave heating on zeolite dehydration. This also motivate the investigation on water adsorption and microwave dehydration of micrometer-thickness zeolites, for instance, if the thickness decreases from 8 μm to 800 nm, we assume the time consumed for hydration and dehydration would be reduced by at least several order of magnitudes. Though it is hard to be proved experimentally, simulations were done by our collaborator to offer the evidence on how fast the water molecules can transfer its energy to zeolite under 360 K and 440 K, which are all at picoseconds level (Figure 2.17).

Overall, the water adsorption and desorption of zeolite NaY has been explored from various aspects. The kinetics of the water adsorption shows NaY is an excellent desiccant though commercial binders in the NaY pellets affect the initial adsorption rate greatly. Neutron images were taken to reveal the spatial water diffusion and adsorption/desorption pattern, the consideration arises that as the thickness of NaY particles decrease greatly (e.g., to micrometer level), the water adsorption and desorption can happen at an extremely high speed, which is time and energy saving and can be utilized in industry techniques. Also, solid-state NMR spectra were measured to show the interactions of water molecules and zeolite framework. And there is an agreement with the theoretical calculations and simulations. Microwave and hot N_2 heating were evaluated as conventional and novel way for zeolite dehydration. The exploration of the hydration and dehydration process can optimize the applications of zeolite in industries. At the same time, it inspires the study on the modification of synthesized NaY for the goal of time and energy conserving, especially for industry techniques and devices.

References

1. Maltesen, M. J.; van de Weert, M., Drying methods for protein pharmaceuticals. *Drug Discov Today Technol* **2008,** *5* (2-3), e81-8.
2. Farag, H. A. A.; Ezzat, M. M.; Amer, H.; Nashed, A. W., Natural gas dehydration by desiccant materials. *Alexandria Engineering Journal* **2011**, 50 (4), 431-439.
3. K.C. Ng, H.T. Chua, C.Y. Chung, C.H. Loke, T. Kashiwagi, A. Akisawa, B.B. Saha, Experimental investigation of the silica gel–water adsorption isotherm characteristics, *Applied Thermal Engineering*, **2001**, 21, 1631-1642,
4. Desiccant Chart Comparisons, https://www.sorbentsystems.com/desiccants_charts.html, accessed Oct.24, 2021
5. S Sircar. Basic Research Needs for Design of Adsorptive Gas Separation Processes, *Ind. Eng. Chem. Res.* **2006,** *45,* 5435-5448
6. Furukawa, H.; Gandara, F.; Zhang, Y. B.; Jiang, J.; Queen, W. L.; Hudson, M. R.; Yaghi, O. M., Water adsorption in porous metal-organic frameworks and related materials. *J Am Chem Soc* **2014,** *136* (11), 4369-81.
7. Luo, Y.; Tan, B.; Liang, X.; Wang, S.; Gao, X.; Zhang, Z.; Fang, Y., Dry Gel Conversion Synthesis of Hierarchical Porous MIL-100(Fe) and Its Water Vapor Adsorption/ Desorption Performance. *Industrial & Engineering Chemistry Research* **2019**, 58 (19), 7801-7807.
8. Yousheng T, Hiroyuki M, Morinobu E, and Katsumi K, Evidence of Water Adsorption in Hydrophobic Nanospaces of Highly Pure Double-Walled Carbon Nanotubes, *J. Am. Chem. Soc.* **2010**, 132, 4, 1214–1215
9. LaPotin, A.; Kim, H.; Rao, S. R.; Wang, E. N., Adsorption-Based Atmospheric Water Harvesting: Impact of Material and Component Properties on System-Level Performance. *Acc Chem Res* **2019,** *52* (6), 1588-1597.
10. Shah, M. S.; Tsapatsis, M.; Siepmann, J. I., Hydrogen Sulfide Capture: From Absorption in Polar Liquids to Oxide, Zeolite, and Metal-Organic Framework Adsorbents and Membranes. *Chem Rev* **2017,** *117* (14), 9755-9803.
11. Meier, W.M., Olson, D.H. Atlas of Zeolite Structure Types, 4th ed. (ed. Elsevier Science). London, **1996**, pp405
12. Sharma, P.; Song, J. S.; Han, M. H.; Cho, C. H., GIS-NaP1 zeolite microspheres as potential water adsorption material: Influence of initial silica concentration on adsorptive and physical/topological properties. *Sci Rep* **2016,** *6*, 22734.
13. Stach H, Mugele J, Jänchen J, Weiler E. Influence of cycle temperatures on the thermochemical heat storage densities in the systems water/microporous and water/mesoporous adsorbents. *Adsorption*, **2005**, 11(3-4): 393–404
14. Wang Y, LeVan M D. Adsorption equilibrium of carbon dioxide and water vapor on zeolites 5A and 13X and silica gel: pure components. *Journal of Chemical & Engineering Data*, **2009**, 54(10): 2839–2844
15. Bahraminia, S.; Anbia, M.; Koohsaryan, E., Dehydration of natural gas and biogas streams using solid desiccants: a review. *Frontiers of Chemical Science and Engineering* **2021,** *15* (5), 1050-1074.
16. R. Caicedo-Realpe, J. P´erez-Ramírez, Mesoporous ZSM-5 zeolites prepared by a two-step route comprising sodium aluminate and acid treatments, *Microporous Mesoporous Mater.* **2010**, 128, 91–100

17. A. Risti´c, F. Fischer, A. Hauer, N. Zabukovec Logar, Improved performance of binder-free zeolite Y for low-temperature sorption heat storage, *J. Mater. Chem*. **2018**, 6, 11521–11530.
18. J.C. Moı¨se, J.P. Bellat, A. M´ethivier, Adsorption of water vapor on X and Y zeolites exchanged with barium, *Microporous Mesoporous Mater*. **2001**, 43, 91–101.
19. Auerbach, S.M., Carrado, K.A., & Dutta, P.K. Handbook of Zeolite Science and Technology (1st ed.). Boca Raton, **2003**.
20. Ryu, Y.K., Lee, S.J., Kim, J.W. et al. Adsorption equilibrium and kinetics of H_2O on zeolite 13x. *Korean J. Chem. Eng*. **2001**, 18, 525–530.
21. Warren, J. M.; Bilheux, H.; Kang, M.; Voisin, S.; Cheng, C.-L.; Horita, J.; Perfect, E., Neutron imaging reveals internal plant water dynamics. *Plant and Soil* **2013,** *366* (1-2), 683-693.
22. Terreni, J.; Trottmann, M.; Delmelle, R.; Heel, A.; Trtik, P.; Lehmann, E. H.; Borgschulte, A., Observing Chemical Reactions by Time-Resolved High-Resolution Neutron Imaging. *The Journal of Physical Chemistry C* **2018**, 122 (41), 23574-23581.
23. Jiri Cejka, Herman van Bekkum, A. Corma, F. Schueth, Introduction to Zeolite Molecular Sieves, 3rd ed, (ed. Elsevier). **2007**, chapter 12.
24. J acek Klinowski, Applications of solid-state NMR for the study of molecular sieves, *Analytica Chimica Acta*,**1993**, 283, 929-965.
25. Shigenobu Hayashi, Solid-state NMR study of locations and dynamics of interlayer cations and water in kanemite, *J. Mater. Chem.*, **1997**, 7(6), 1043–1048
26. Jin-Fu Wu, Tun-Li Chen, Long-Ja Ma, May-Whei Lin, Shang-Bin Liu, N.m.r. investigation of benzene adsorption on a dehydrated NaY zeolite, Zeolites, 1992, 12, 86-94.
27. Alberti, A., Cariati, F., Erre, L., Piu, P., and Vezzalini, G. Spectroscopic investigation on the presence of OH in natural barrerite and in its collapsed phases. *Physics and Chemistry of Minerals*, **1983**, 9, 189-191.
28. F.E Trigueiro, D.F.J Monteiro, F.M.Z Zotin, E Falabella Sousa-Aguiar, Thermal stability of Y zeolites containing different rare earth cations, *Journal of Alloys and Compounds*, **2002**, 344, 337-341
29. Prokof'ev, V.Y., Gordina, N.E., Zakharov, O.N. *et al.* Study of the Kinetics of Adsorption and Desorption of Water Vapor on Low-Silica Zeolites. *Pet. Chem.* **2020**, 60, 550–556.
30. Dinesh K Agrawal, Microwave processing of ceramics, *Current Opinion in Solid State and Materials Science*, **1998**, 3(5), 480-485
31. Ohgushi, T., Komarneni, S., Bhalla, A.S. Mechanism of Microwave Heating of Zeolite A. *Journal of Porous Materials* **2001**, 8, 23–35.
32. Chan, KC, Chao, CYH, & Bahrami, M. Heat and Mass Transfer Characteristics of a Zeolite 13X/CaCl2 Composite Adsorbent in Adsorption Cooling Systems. ASME 2012 6th International Conference on Energy Sustainability, Parts A and B. San Diego, California, USA. July 23–26, **2012**. 49-58.

Chapter 3 Exploration of composites combining zeolite NaY with other type of materials

3.1 Introduction

In today's research, engineering micro arrangements of pure substances and composite materials is becoming increasingly important not only in the development of elaborate water adsorption materials, but also in novel molecular level electrical, optical, catalytic, and magnetic devices. One attracted topic is assembling microlevel structures to various substrate or templates. Many approaches have been explored to create the novel composites and applied for a variety of reactions and applications. According to previous studies, silicon nanoparticles dispersed uniformly between two layers of graphene sheets has been developed using the electrostatic attraction directed self-assembly method, the synthesized Si-NP@graphene nanocomposite shows improved performance for lithium-ion batteries.[1] Labeling Gold nanoparticles (AuNPs) utilizing single stranded DNA (ssDNA) could be applied to build multimeric networks and chain-like forms through with sequence-specific DNA hybridization.[2,3] This approach has been used for the linear assembling of AuNPs which have controlled spatial arrangement.[3] Moreover, using self-assembly method, the assembled composite of ZnO nanoparticles in mesostructured SnO_2 was obtained by preparing ZnO nanoparticles in the pores of mesostructured SnO_2, and it was found the photoluminescence intensity of the composite is more than fivefold of the nanometer ZnO in green and ultraviolet range.[4] Recently, hybrid poly (methyl methacrylate) (PMMA) / reduced graphene oxide/Fe_2O_3 nanocomposites was obtained using in-situ polymerization fabrication, the outstanding thermal conductivity, dielectric, and mechanical properties were exhibited.[5] Co/ZSM-5@Silicalite-1 composites were made using zeolite ZSM-5 as support and Co as the core, zeolite silicate-1 was fabricated as the shell covered on the top.[6] Analysis was done based on the pivotal functions of zeolite in fuel chemistry, Co/ZSM-5@Silicalite-1 shows high gasoline selectivity. Fe based

nanoparticles-zeolite composites were found as an efficient material for the cesium removal from liquid, possibly can be applied for wastewater treatment.[7]

In the past two decades, the fabrication of aluminosilicate or zeolite with other type of substrates to form composites has been explored for various applications. Polypropylene–zeolite composites were made with different zeolite mass loading (6–40 wt.%) for water adsorption test.[8] Maghemite-zeolite Y magnetic composites exhibits adsorption ability of chromate, which can be utilized in sewage treatment and environmental protection applications.[9] Chemical approaches for assembling zeolite thin films on substrates can be divided into two categories: direct growth and post synthetic crystal attachment.[10,11,12] The direct growth usually done by the in situ zeolite particles growth on the substrates which are immersed in the synthesis gel. The first example of oriented zeolite particle in situ growth attachment was done by S. Feng and T. Bein, who successfully combined zinco-phosphate zeolite with the organophosphate multilayer films modified gold substrates.[13] The catalytic functions of trans alkylation and alkylation of benzene reactions were evaluated using variformed alumina supports coated MFI and BEA type of zeolite particles, in which the in situ growth was studied and applied.[14] Specially, high-silica zeolite UTD-1 were oriented onto polished silicon wafers by pulsed laser ablation followed by hydrothermal treatment immersing in the UTD-1 synthesis gel.[15] As stated, in most cases, the substrates or films are chemically prepared or modified using colloidal seeding gel for better coating. While for post synthetic attachment, zeolite particles would be chemically assembled to the substrate or film through hydrogen bonding, covalent bonding, and ionic bonding using various bridging organic molecules.

Polyamines were used as powerful molecular ligament to assemble monolayer zeolite crystals onto glass using dendritic polyamine (DPA) and polyethyleneimine (PEI) as the linkage.[16] Zeolite A

and ZSM-5 monolayers were assembled to glass surface by using aminopropyl silyl tethered to zeolite surface and [3-(2,3-epoxypropoxy) propyl] trimethoxy silane tethered to glass surface in toluene solvent.[17] Fullerene was also used as the covalent bridging molecule to assemble zeolite particles on glass surface.[18] Additionally, trimethyl propylammonium iodide tethered zeolite ZSM-5 and sodium butyrate tethered glass was combined through ionic bonding.[19] ZSM-5 and zeolite A monolayers were attached to glass via adenine-thymine hydrogen bonding.[20] Various linkages have been collected and reported by Yoon group,[21] as shown in Figure 3.1. Glass plates are ideal substrate for zeolite particle attachment for their smooth surface and liability to be modified. In addition, using glass as the substrate has good feasibility, since the microwave would be a potential novel way for zeolite dehydration and recycle based on previous discussion. Given the dielectric constant of vacuum was set to 1.0, generally the dielectric constant of common glass is lower than 10, which is exceedingly low compared to 80 of water and almost infinite of metals. Furthermore, the attachment of zeolite NaY to glass hasn't been studied a lot because of the less symmetry of NaY structure. Based on bibliography of the ultrasound assisted assembly of silicalite crystals onto 3-halopropyl tethered glass plates reported by Yoon group,[22] the attachment of synthesized zeolite NaY onto glass slides was explored in this experiment.

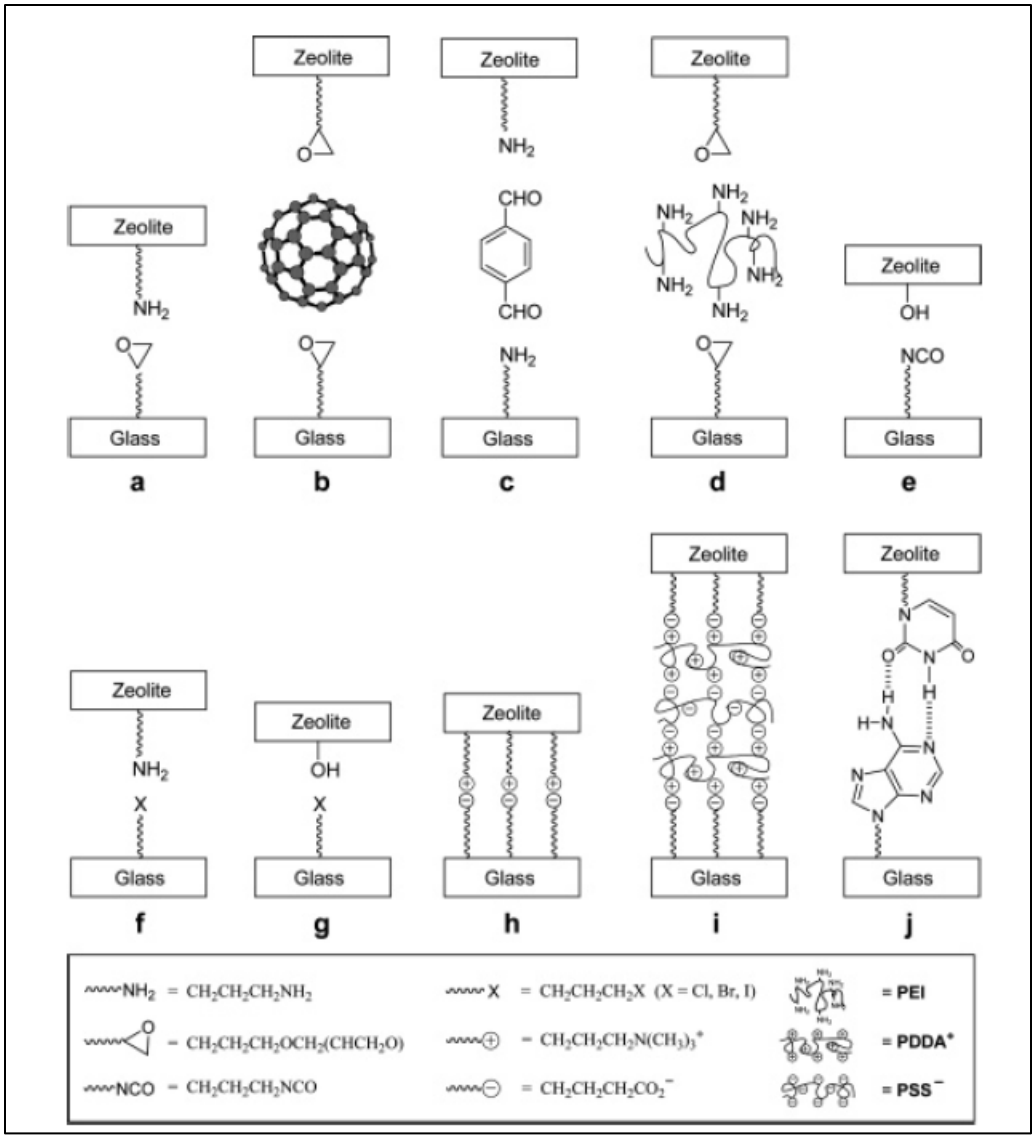

Figure 3.1. Zeolite assembled on glass using different types of molecular linkages.[21] Reproduced with permission from Yoon.

Besides, it is reported that zeolite particles can also be assembled onto glass surface based on physical adsorption. Convective assembly of zeolite ZSM-2 by evaporation aided withdrawal coating to hexagonal nanoplates was achieved by Tsapatsis Group.[23] Using dip-coating method, zeolite particles with homogeneous nucleation were attached to glass substrates.[24,25] Related investigations are provoked that if zeolite NaY can be attached to other type of commonly used

material use dip-coating method and if the dip-coating method can be further modified to meet common applications.

Polyurethanes (PU) were developed in 1930-1940s by Otto Bayer,[26] which is made by combining di-isocyanates and polyols and has become one of the most popular plastic polymers in recent decades. It has wide applications in daily and industrial use, ranging from insulations in the freezer and buildings, to the coatings on the furniture and aero planes. The recent work on composites of PU and various particles/crystals shows the wide potential of PU composites. TiO_2 nanoparticle/polyurethane (TPU) composite was synthesized and used as the substrate to be modified with tetradecyl amine (TDA)-amidated graphene oxide (GO-TDA), the final composite TPU-GO-TDA foam exhibits excellent performance in oil spill cleanup,[27] which could benefit water treatment and marine pollution. Hydroxyapatite/silver nanoparticles coated polyurethane scaffold composite was obtained and it shows antibacterial properties.[28] Variety of reinforced PU composite also been reported in the past two decades. The fumed SiO_2 particle filled PU foam was synthesized and it has improved compressive strength.[29] Calcium copper titanate/polyurethane composite film was obtained, and it extremely exhibits flexibility and high dielectric constant.[30] However, there is few studies on zeolite and PU composite. Zeolite beta has been used to improve mechanical properties of PU.[31] Different weight percent of zeolite 13X also been fabricated to form PU/zeolite 13X nanocomposite films which has promoted mechanical and thermal properties.[32] Though, zeolite particles mainly were used as the filler for PU structure, and there's no previous work has been done on incorporating Faujasite particles to PU. The composite of NaY/PU has been synthesized and it could possibly be used for various areas including water adsorption because of the relatively low dielectric constant of PU materials.

3.2 Experimental

NaY-Glass attachment

The procedures for zeolite NaY (average size 350 nm) synthesis can be found in the first part. 3-Chloropropyltrimethoxysilane (CP-TMS, Sigma-Aldrich) was used as received without further purification. Glass slides (round cover glass) were cleaned and hydroxylated by freshly made piranha solution for 1 h. Then, the glass surface was cleaned by deionized water followed by drying under argon. Glass slides were immersed in the 20 mL of toluene (anhydrous, 99.8%, Sigma-Aldrich) solution of CP-TMS (0.1 M) and refluxed under argon for at least 4 h. The CP-TMS tethered glass plates mounted on the lab made PTFE support and the crystals of dried zeolite were introduced into toluene (20 mL) in a 50 mL beaker. The solution was sonicated for 2 min. Samples were analyzed by scanning electron microscopy (SEM, Scios 2 DualBeam). Images were acquired by Dr. Lien.

NaY-PU attachment

The synthesis of Polyurethane foam was modified based on bibliography.[33] Polycaprolactone triol (PCLt, average Mn ~300, Sigma-Aldrich) and Polyethylene glycol (PEG, Sigma-Aldrich) were mixed into a polypropylene beaker under 55℃ water bath with mechanical stirring. Then, silicone oil (Sigma-Aldrich), N, N-dimethyl benzylamine (Fisher Scientific), dibutyltin dilaurate (for synthesis level, Sigma-Aldrich) and deionized water were added after few minutes. Hexamethylene diisocyanate was (for synthesis level, Sigma-Aldrich) was added to the above mixture under vigorous stirring. The mixture reached the polymer cream time after 20 seconds of stirring. The stirring was stopped and removed; the foam would form in few seconds. Then the foam was cured under 55 ℃ for 1h and under room temperature for 24 h to remove toxicity. The

molar composition of synthesis mixture was PCLt: PEG: silicone oil: N, N-dimethyl benzylamine: dibutyltin dilaurate: water: hexamethylene diisocyanate = 50: 50: 1.9: 0.3: 0.8: 10: 119.

Then, the freshly made PU and 0.1 M (3-Aminopropyl) triethoxysilane (APTES, >99%, Sigma-Aldrich) was put into the container with ethanol as solvent. The reaction was set under room temperature for 24 h. Then, 100 mg of 200 ℃ dried as-synthesized zeolite NaY particles was sonicated in ethanol solution until no aggregation. The modified PU pieces were washed with ethanol and then transferred into NaY solution and react for 1 h under room temperature. Control experiment was done without APTES modification. Samples were analyzed using scanning electron microscopy (SEM, Scios 2 DualBeam). And images were acquired by Dr. Lien.

NaY-PU-Fiberglass attachment

Household fiberglass with 80% openness was purchased from Home Vibes company. Physical attachment of NaY particle was obtained by dip coating. NaY particles was sonicated in ethanol until the solution is uniform. Cleaned fiberglass pieces were immediately dip in the solution and dried. Then the dip coating process was repeated for 4 times.

"Pseudo dip coating" was done by using PU film prepared by dissolving Poly [4,4′-methylene bis (phenyl isocyanate)-alt-1,4-butanediol/di (propylene glycol)/polycaprolactone] pellets (Sigma-Aldrich) in anhydrous tetrahydrofuran (THF, Sigma-Aldrich) under room temperature for at least 24 h. Then, cleaned fiberglass screens were dip in PU solution and take out. Before the PU foam is completely formed, the PU-film coated fiberglass was dip in the freshly sonicated zeolite NaY particles in THF solvent again. Then the NaY-PU-Fiberglass composite were cured for 24 h under room temperature. Samples were analyzed by scanning electron microscopy (SEM, Scios 2 DualBeam). Images were acquired by Dr. Lien.

3.3 Results and discussion

NaY-Glass attachment

The NaY-Glass composite was obtained using CP-TMS as the linking molecule, trimethyl group bonded glass could link to hydroxyl bonded zeolite by a direct nucleophilic substitution of terminal chloride. Pictures of bare glass slides and NaY coated glass slides were took as shown in Figure 3.2, in which the huge difference of before and after modification was noticed. Degree of coverage (DOC) has been used to evaluate the coating on the substrate. SEM images were took as shown in Figure 3.3, the DOC around 90% was obtained in our experiment using sonication aided reaction, the monolayer attachment was observed. The traditional heating and reflux procedure which took at least 4 h also been used to replace the sonication step, though a lower coverage (60%) was observed, as shown in Figure 3.4. Longer reaction time might be needed for a better attachment for NaY particles, though it's not preferable due to the large energy and time consumption. Thus, the sonication aided method can assist to get better zeolite particle coverage efficiently in 2 min, and the first reported Faujasite NaY particle attached glass NaY-Glass was successfully obtained in this experiment. Moreover, the glass material is microwavable, which means NaY-Glass materials can be dehydrated through microwave after hydration. Though the kinetics of adsorption is hard to measure without well-designed instrument since the energy transfer of water with monolayer NaY will happen in picoseconds, still NaY-Glass is a promising dehydration composite with excellent reusability, also it may be applied in catalytic reactions and insulation use with further study.

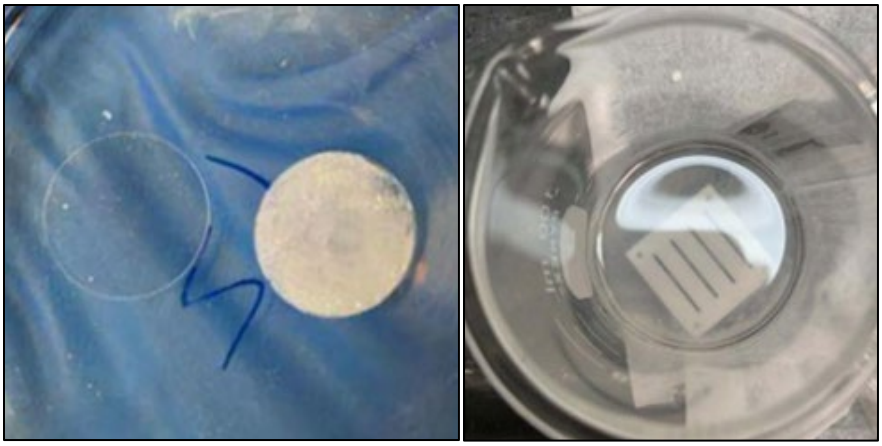

Figure 3.2. Left: the comparison of bare round glass slide and NaY coated glass. Right: Lab designed PTFE mount to hold the glass slides under sonication.

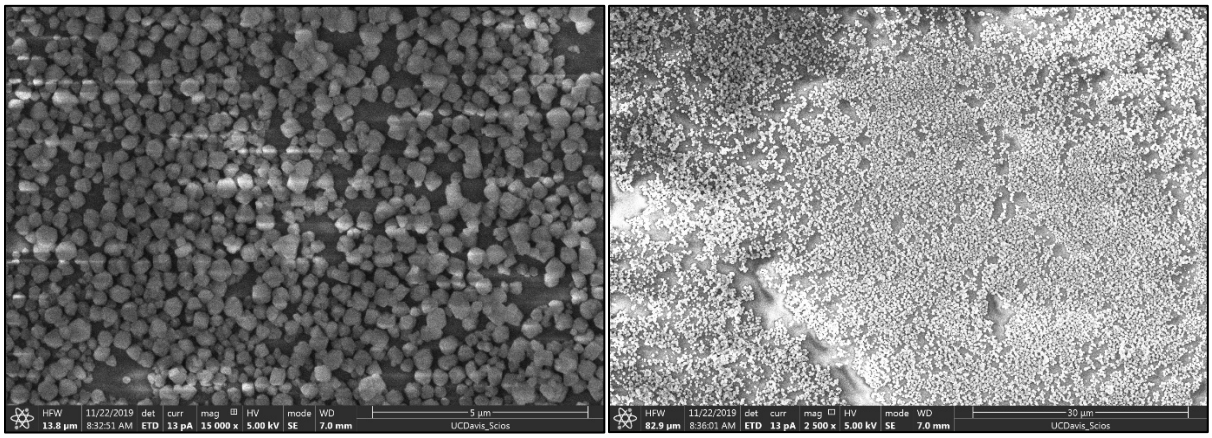

Figure 3.3. SEM images of sonication aided NaY-Glass attachment samples.

NaY-PU attachment

Fiberglass is considered as an ideal substrate due to its low cost and wide applications, in addition, it is non-magnetic, non-conductive, and transparent to electromagnetic radiation, which make it a promising material for microwave substrate. To mount NaY particles onto a piece of fiberglass, the physical attachment was achieved by using dip coating method as mentioned. A good attachment can be observed, and the 20 wt.% mass increases can be noticed. Based on the microwave safety of fiberglass, this composite can be used as a reusable multifunctional air filter

for water adsorption, gas separation, waste treatment and some catalytic reactions. However, the physical attached particles may fall off easily when other substances pass through, which limits the utility of the composite.

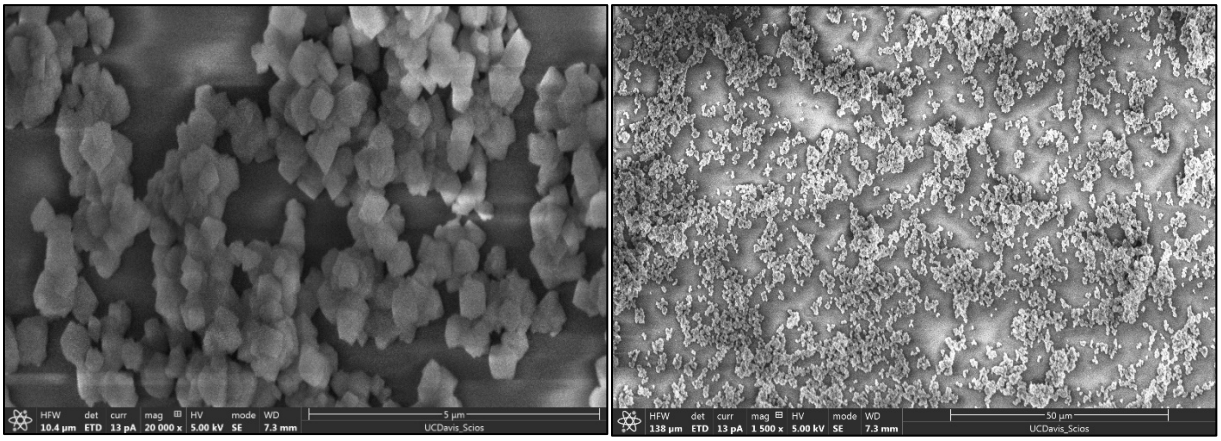

Figure 3.4. SEM images of NaY-Glass attachment samples using reflux and heating procedure, a less coverage 60± 5 % was observed.

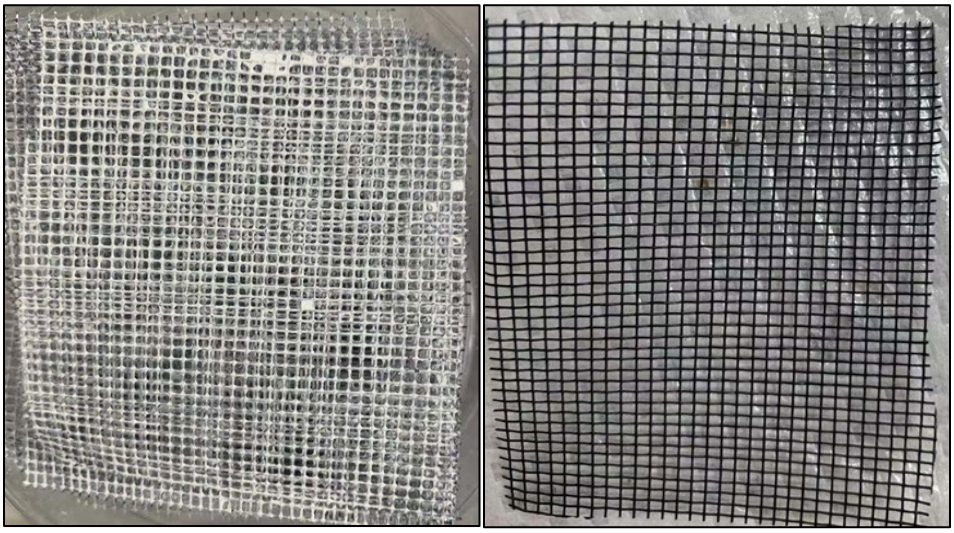

Figure 3.5. Pictures of NaY attached fiberglass(left) and bare fiberglass(right).

To solve this problem, a polymeric substrate PU foam was used to replace the fiberglass, APTES was used as the binder between PU and NaY crystals. Zeolite contained polymer usually exhibits

better mechanical and thermal properties. APTES can combine polyurethane structure with NaY particles through covalent bonding which is stabler than physical attachment. And to confirm the function of APTES, a control experiment was done without silane as the bridging molecule, Figure 3.6 shows the comparison of two types of samples. For the reaction with APTES added, a multilayer coverage larger than 80% was obtained. The coverage was low for the control experiment, and there's only few particles attached, which is mainly due to the hydrogen bonding. In Figure 3.7, the possible bonding between PU and zeolite particles was proposed by previous literature[34] for the zeolite SAPO-5 filled polyurethane membrane. The NCO group and hydroxyl group of PU can attach hydroxyl bonded zeolite mainly via hydrogen bonding. The comparison suggests APTES can elevate the attachment greatly, however, the coverage is not uniform, and a bumpy surface was noted. This might attribute to the fast aggregation of zeolite particles and the surface, which is not smooth enough, other smoother substrate or the alleviation of agglomeration, can possibly solve the problem.

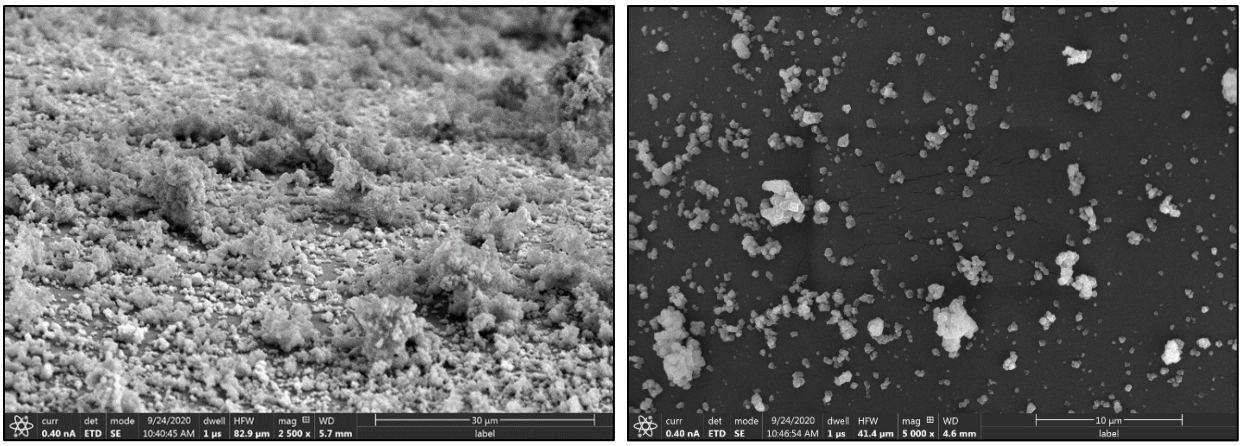

Figure 3.6. SEM images of NaY-PU sample use APTES (left) as the linkage and control experiment sample without APTES.

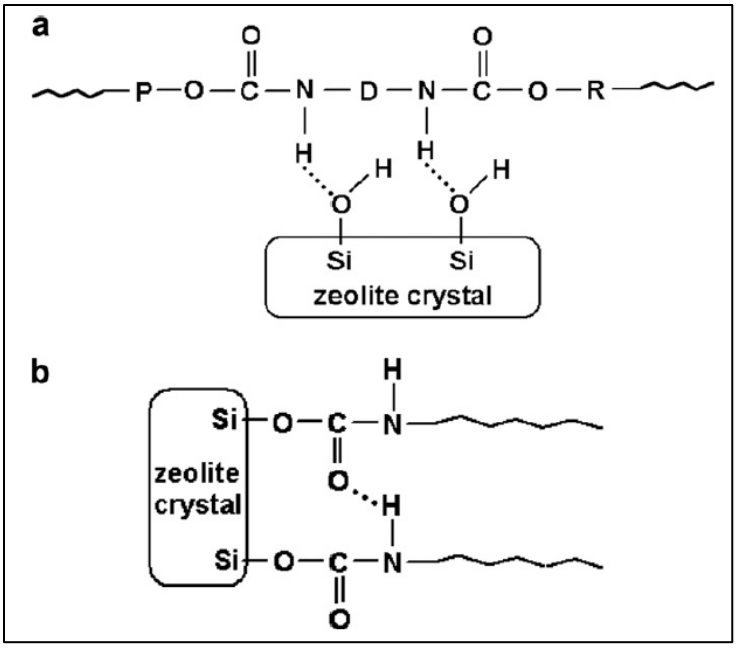

Figure 3.7. Proposed hydrogen bonding in the SAPO-5 filled polyurethane membrane.[34] Reproduced with permission from Nicolais, Iannace and Alfani.

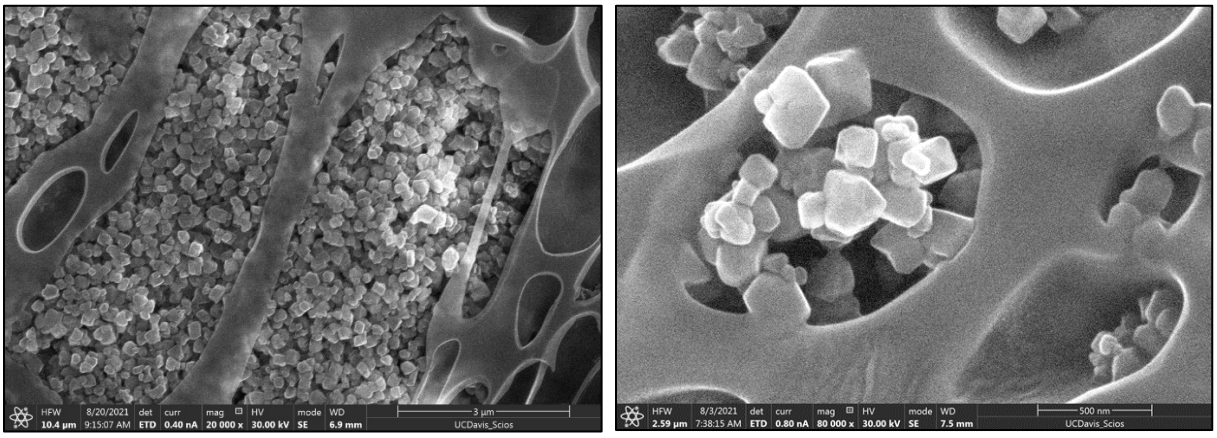

Figure 3.8. SEM images of NaY-PU-Fiberglass samples.

NaY-PU-Fiberglass attachment

To explore more possibilities of composites containing NaY particles, PU film was made as mentioned to serve as a binder between fiberglass and zeolite. The experiment was inspired by the previous study[35] that doctor-blade method was utilized to make MOF (ZIF-8)-PU composite. Though in this experiment, doctor-blade method is not applicable owing to the unsmooth surface. Instead, a pseudo dip-coating procedure was designed to create a close packed NaY particles coating through PU film. As stated, the fiberglass was immersed in the PU solution and then set for vaporization, then a viscous PU film would form. And it has the affinity to coat on another substrate surface, the PU film enfold the fiberglass tightly. The PU-Fiberglass was immersed in the sonicated zeolite solution subsequently, and the hydrogen bonding between PU membrane and zeolite particles would grasp the zeolite onto the PU membrane. SEM images in Figure 3.8 show the good coverage and close packing of zeolite particles and indicate the linkage between PU membrane and zeolite. Because of the microwave safety of PU membrane and fiberglass, the NaY-PU-Fiberglass composite could be used as a reusable drying filter, the humid air can pass through the screen while the water would be adsorbed quickly by the multi-layer zeolite attached. Besides, due to the viscosity of PU film before fully dried, PU film can be used to coat zeolite onto variety type of substrates such as PTFE, carbon nanotube and metal surface. The methodologies we designed can be utilized into extended energy-conserving materials and applications, which deserve more investigations.

References

1. Zhou, X.; Yin, Y.-X.; Wan, L.-J.; Guo, Y.-G., Self-Assembled Nanocomposite of Silicon Nanoparticles Encapsulated in Graphene through Electrostatic Attraction for Lithium-Ion Batteries. *Advanced Energy Materials* **2012**, 2 (9), 1086-1090.
2. C. A. Mirkin, R. L. Letsinger, R. C. Mucic and J. J. Storhoff, A DNA-based method for rationally assembling nanoparticles into macroscopic materials*Nature*, **1996**, 382, 607–609
3. Deng, Z.; Tian, Y.; Lee, S. H.; Ribbe, A. E.; Mao, C., DNA-encoded self-assembly of gold nanoparticles into one-dimensional arrays. *Angew Chem Int Ed Engl* **2005**, 44 (23), 3582-3585.
4. Yude, W.; Shuo, Z.; Xinghui, W.; Qingju, L., Synthesis and optical properties of nano-ZnO particles/mesostructured SnO_2 composite. *Materials Chemistry and Physics* **2006**, 98 (1), 121-124.
5. Ul-Haq, Y.; Murtaza, I.; Mazhar, S.; Ullah, R.; Iqbal, M.; Zeeshan ul, H.; Qarni, A. A.; Amin, S., Dielectric, thermal and mechanical properties of hybrid PMMA/RGO/Fe2O3 nanocomposites fabricated by in-situ polymerization. Ceramics International 2020, 46 (5), 5828-5840.
6. Javed, M.; Cheng, S.; Zhang, G.; Dai, P.; Cao, Y.; Lu, C.; Yang, R.; Xing, C.; Shan, S., Complete encapsulation of zeolite supported Co based core with silicalite-1 shell to achieve high gasoline selectivity in Fischer-Tropsch synthesis. *Fuel* **2018**, 215, 226-231.
7. Eljamal, O.; Shubair, T.; Tahara, A.; Sugihara, Y.; Matsunaga, N., Iron based nanoparticles-zeolite composites for the removal of cesium from aqueous solutions. *Journal of Molecular Liquids* **2019**, 277, 613-623.
8. Pehlivan, H., Özmıhçı, F., Tıhmınlıoğlu, F., Balköse, D. and Ülkü, S., Water and water vapor sorption studies in polypropylene–zeolite composites. *J. Appl. Polym. Sci.*, **2003**, 90, 3069-3075.
9. Barquist, K.; Larsen, S. C., Chromate adsorption on bifunctional, magnetic zeolite composites. *Microporous and Mesoporous Materials* **2010**, 130 (1-3), 197-202.
10. Thomas Bein, Synthesis and Applications of Molecular Sieve Layers and Membranes, *Chem. Mater*. **1996**, 8, 8, 1636–1653.
11. Z. Li, C. Lai, T. E. Mallouk, Self-Assembling Trimolecular Redox Chains at Zeolite Y Modified Electrodes *Inorg. Chem*. **1989**, 28, 178 - 182.
12. T. Munoz, Jr., K. J. Balkus, Jr., Preparation of Oriented Zeolite UTD-1 Membranes via Pulsed Laser Ablation *J. Am. Chem. Soc*. **1999**, 121, 139 -146
13. Feng, S., Bein, T. Growth of oriented molecular sieve crystals on organophosphonate films. *Nature* **1994**, 368, 834–836.
14. N van der Puil, F.M Dautzenberg, H van Bekkum, J.C Jansen, Preparation and catalytic testing of zeolite coatings on preshaped alumina supports, *Microporous and Mesoporous Materials*, **1999**, 27(1), 95-106.
15. Kenneth J. Balkus, Trinidad Muñoz, Mary E. Gimon-Kinsel Preparation of Zeolite UTD-1 Films by Pulsed Laser Ablation: Evidence for Oriented Crystal Growth *Chem. Mater.* **1998**, 10, 2, 464–466.
16. Kulak, A.; Park, Y. S.; Lee, Y.-J.; Chun, Y. S.; Ha, K.; Yoon, K. B., Polyamines as Strong Molecular Linkers for Monolayer Assembly of Zeolite Crystals on Flat and Curved Glass. *J. Am. Chem. Soc*. **2000**, 122 (38), 9308-9309.

17. Alexander Kulak, Yun-Jo Lee, Yong Soo Park, Kyung Byung Yoon, Orientation-Controlled Monolayer Assembly of Zeolite Crystals on Glass and Mica by Covalent Linkage of Surface-Bound Epoxide and Amine Groups, *Angew. Chem*. 2000, 112, 980-983
18. Choi, S. Y.; Lee, Y.-J.; Park, Y. S.; Ha, K.; Yoon, K. B., Monolayer Assembly of Zeolite Crystals on Glass with Fullerene as the Covalent Linker. *J. Am. Chem. Soc*. **2000,** 122 (21), 5201-5209.
19. Lee, G. S.; Lee, Y.-J.; Yoon, K. B., Layer-by-Layer Assembly of Zeolite Crystals on Glass with Polyelectrolytes as Ionic Linkers. *J. Am. Chem. Soc*. **2001,** 123 (40), 9769-9779.
20. Park JS, Lee GS, Lee YJ, Park YS, Yoon KB. Organization of microcrystals on glass by adenine-thymine hydrogen bonding. *J. Am. Chem. Soc*. **2002**, 124, 13366-13367
21. Yoon, K. B., Organization of Zeolite Microcrystals for Production of Functional Materials. Acc. Chem. Res. **2007**, 40, 1, 29–40
22. Lee, J. S.; Ha, K.; Lee, Y. J.; Yoon, K. B., Ultrasound-Aided Remarkably Fast Assembly of Monolayers of Zeolite Crystals on Glass with a Very High Degree of Lateral Close Packing. *Advanced Materials* **2005**, 17 (7), 837-841.
23. Choi, J.; Lai, Z.; Ghosh, S.; Beving, D. E.; Yan, Y.; Tsapatsis, M., Layer-by-Layer Deposition of Barrier and Permselective c-Oriented-MCM-22/Silica Composite Films. *Industrial & Engineering Chemistry Research* **2007,** *46* (22), 7096-7106.
24. Lee, J. A.; Meng, L.; Norris, D. J.; Scriven, L. E.; Tsapatsis, M., Colloidal Crystal Layers of Hexagonal Nanoplates by Convective Assembly. *Langmuir* **2006**, 22 (12), 5217-5219.
25. Lovallo, M.C., Gouzinis, A. and Tsapatsis, M., Synthesis and characterization of oriented MFI membranes prepared by secondary growth. *AIChE J.*, 1998, 44, 1903-1913.
26. Ban, T., Ohwaki, T., Ohya, Y. and Takahashi, Y., Preparation of a Completely Oriented Molecular Sieve Membrane. *Angewandte Chemie International Edition* **1999**, 38, 3324-3326.
27. Otto Bayer, Das Di-Isocyanat-Polyadditionsverfahren (Polyurethane), *Angewandte Chemie.* **1947,** 59 (9), 257–272.
28. Wei, Q.; Oribayo, O.; Feng, X.; Rempel, G. L.; Pan, Q., Synthesis of Polyurethane Foams Loaded with TiO2 Nanoparticles and Their Modification for Enhanced Performance in Oil Spill Cleanup. *Industrial & Engineering Chemistry Research* **2018,** *57* (27), 8918-8926.
29. Ciobanu, G.; Ilisei, S.; Luca, C., Hydroxyapatite-silver nanoparticles coatings on porous polyurethane scaffold. *Mater Sci Eng C Mater Biol Appl* **2014**, 35, 36-42.
30. Huang, W.; Xu, H.; Fan, Z.; Ao, Y.; Liu, J., Compressive response of composite ceramic particle-reinforced polyurethane foam. *Polymer Testing* **2020**,87, 106514.
31. Wan, W.; Luo, J.; Huang, C.-e.; Yang, J.; Feng, Y.; Yuan, W.-X.; Ouyang, Y.; Chen, D.; Qiu, T., Calcium copper titanate/polyurethane composite films with high dielectric constant, low dielectric loss and super flexibility. *Ceramics International* **2018**, 44 (5), 5086-5092.
32. Aksoy, E. A.; Akata, B.; Bac, N.; Hasirci, N., Preparation and characterization of zeolite beta–polyurethane composite membranes. *Journal of Applied Polymer Science* **2007**, 104 (5), 3378-3387.
33. Ghobadi, E.; Hemmati, M.; Khanbabaei, G.; Shojaei, M.; Asghari, M., Effect of nanozeolite 13X on thermal and mechanical properties of Polyurethane nanocomposite thin films. *International Journal of Nano Dimension* **2015**, 6 (2), 177-181.
34. Alfani, R., Iannace, S. and Nicolais, L., Synthesis and characterization of starch-based polyurethane foams. *J. Appl. Polym. Sci.***1998**, 68, 739-745.

35. Hassan Sharifi Pajaie, Majid Taghizadeh. Investigating the Effect of Ultrasonic and Microwave-Assisted Aging on the Synthesis of Nanosized SAPO-34 Molecular Sieves Using Box–Behnken Experimental Design. *Synthesis and Reactivity in Inorganic, Metal-Organic, and Nano-Metal Chemistry* **2016**, 44, 701-712.
36. Mahdi, E. M.; Tan, J.-C., Dynamic molecular interactions between polyurethane and ZIF-8 in a polymer-MOF nanocomposite: Microstructural, thermo-mechanical and viscoelastic effects. *Polymer* **2016,** *97*, 31-43.